Table 1. Changes in survival rate, heart weight/body weight ratio, heart rate, percentage of fibrosis, expression of TGF-β1 and collagen-III mRNA and the hemodynamic parameters in rats with heart failure after treatment with candesartan

	Group-N	Group-V	Group-C0.05	Group-C0.5	Group-C5
Survival rate (%)	100	73*	73*	87	93#
HW/BW (g/kg)	2.5 ± 0.1	3.8 ± 0.2**	3.7 ± 0.2**	3.3 ± 0.1**,#	3.1 ± 0.1**,#
HR (bpm)	311 ± 12	300 ± 13	296 ± 21	291 ± 13	252 ± 8**,#
% fibrosis (%)	3 ± 0.6	32 ± 3.7**	25 ± 2.7**	20 ± 3.0**,##	12 ± 1.4##
TGF-β1 (%)	100	367 ± 26**	349 ± 23**	292 ± 81**,##	204 ± 63**,##
Collagen-III (%)	100	437 ± 18**	395 ± 22**,##	364 ± 42**,##	259 ± 33**,##
CVP (mmHg)	−0.4 ± 0.2	4.1 ± 1.1**	4.0 ± 1.4**	3.0 ± 0.8*	2.0 ± 0.5*
Mean BP (mmHg)	101.5 ± 2.5	77.4 ± 3.4**	69.9 ± 5.9**	80.1 ± 5.3**	64.3 ± 4.9**
LVP (mmHg)	110 ± 3	88 ± 2**	76 ± 5**	88 ± 4**	72 ± 4**
LVEDP (mmHg)	4.3 ± 1.0	13.4 ± 1.0**	13.3 ± 1.1**	8.0 ± 0.9*,##	5.5 ± 1.0##
+dP/dt (mmHg/s)	5564 ± 243	2894 ± 155**	2580 ± 322**	3524 ± 229**	3334 ± 322**
−dP/dt (mmHg/s)	−5002 ± 654	−2916 ± 212**	−2298 ± 311**	−4155 ± 343	−3631 ± 314*

Group-N, normal rats; Group-V, rats with heart failure; Group-C0.05, 0.05 mg/kg candesartan per day; Group-C0.5, 0.5 mg/kg candesartan per day; Group-C5, 5 mg/kg candesartan per day; HW/BW, heart weight/body weight ratio; HR, heart rate; Percentage of fibrosis, area of fibrosis; TGF-β1, expression of transforming growth factor-β1 mRNA; Collagen-III, expression of collagen-III mRNA; CVP, central venous pressure; Mean BP, mean arterial blood pressure; LVP, peak left ventricular pressure; LVEDP, left ventricular end-diastolic pressure.
All values are expressed as the mean ± S.E.M.. $^{*}p < 0.05$ and $^{**}p < 0.01$ versus Group-N, $^{\#}p < 0.05$ and $^{\#\#}p < 0.01$ versus Group-V.

Heart weight/body weight ratio

The heart weight/body weight ratio was increased in Group-V compared with that in Group-N. Candesartan treatment suppressed the increase in that value in a dose-dependent manner (Table 1).

Histopathology

The area of myocardial fibrosis was increased in Group-V compared with that in Group-N. Candesartan treatment suppressed the increase in the fibrotic area in a dose-dependent manner (Table 1).

Myocardial mRNA expression of transforming growth factor-β1 and collagen-III

As shown in Fig. 2 and Table 1, the levels of left ventricular mRNA expression of TGF-β1 and collagen-III were markedly upregulated in Group-V as compared with those in Group-N. Candesartan treatment significantly suppressed increases in expressions of TGF-β1 and collagen-III in a dose-dependent manner (Table 1 and Fig. 2).

Hemodynamic parameters

LVEDP and CVP were increased in Group-V compared with those in Group-N. Candesartan treatment improved both LVEDP and CVP in a dose-dependent manner (Table 1).

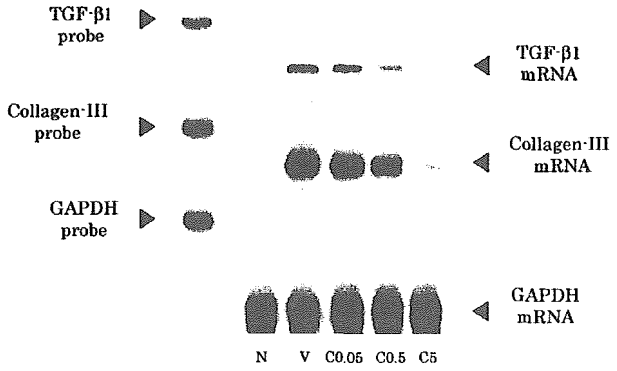

Fig. 2. Left ventricular mRNA expression of transforming growth factor (TGF)-β1 and collagen-III. Although levels of expression of TGF-β1 and collagen-III mRNA were increased in Group-V, they were suppressed by treatment of candesartan in a dose-dependent manner. Left arrows show the probe for target mRNA [TGF-β1, collagen-III, and glyceraldehyde-3-phosphate dehydrogenase (GAPDH)]. Right arrows show the protected band of target mRNA. N, Group-N; V, Group-V; C0.05, Group-C0.05; C0.5, Group-C0.5; C5, Group-C5.

Discussion

A significant part of CHF involves left-ventricular contractile dysfunction and the origin of this dysfunction is mainly referred to two factors; non-ischemic dilated cardiomyopathy

and ischemic heart disease. In this disease, marked hyperdynamics of neuroendocrine factors of the sympathetic system and renin–angiotensin system have been thought to induce progressive dilation and defective contraction of the left-ventricular region; that is, remodeling, followed by events such as exacerbation of heart failure and even death. Thus, recent primary treatment of CHF has involved suppression of left ventricular remodeling via inhibition of these neuroendocrine factors to improve the prognosis of heart failure.

To date, various clinical trials have reported good effects of candesartan on heart failure. Recently, the CHARM trial suggested that candesartan was generally well tolerated and reduced cardiovascular mortality and morbidity in patients with symptomatic chronic heart failure and intolerance of ACEI [19]. Furthermore, the addition of candesartan to ACEI and other treatment leads to a further clinically important reduction in relevant cardiovascular events in patients with CHF and reduced left-ventricular ejection fraction [11]. And finally, candesartan has a moderate impact in preventing admissions for CHF among patients with heart failure and left-ventricular ejection function higher than 40% [20]. Furthermore, the CHARM-Overall program suggested that candesartan significantly reduced the cardiovascular death rate and overall death rate [10].

In the present study, we used Ang-I to increase the blood pressure because we are planning to compare the beneficial effect of ACEI with ARB in heart failure.

We reported previously that long-term treatment with the ACEI, quinapril decreased heart weight and LVEDP, and increased ±dP/dt in this rat model of dilated cardiomyopathy, and that treatment with the ARB, candesartan 0.5 mg/kg had the same Ang-II blocking effects as quinapril 20 mg/kg [12, 18]. Candesartan 10 mg/kg completely blocked the Ang-II-induced blood pressure increase (Fig. 1). Thus, in this study, using a rat model of dilated cardiomyopathy, we examined the effects of candesartan at doses of 0.05 mg/kg (low dose), 0.5 mg/kg (middle dose), and 5 mg/kg (high dose) on the progression of heart failure, on TGF-β1 and collagen-III mRNA expressions and on myocardial fibrosis. These results indicated that candesartan inhibits Ang-II-induced blood pressure increase, and decreases myocardial fibrosis, and TGF-β1 and collagen-III mRNA expression in a dose-dependently in rats with dilated cardiomyopathy.

Hemodynamic analysis demonstrated that the blood pressure of Group-C0.5 was higher than Group-C0.05 or Group-V. It may be due to amelioration of heart function by candesartan treatment. On the other hand, in Group-C5, the blood pressure was decreased more than Groups-C0.05 and -C0.5. It is supposed that hypotensive effect of high-dose candesartan exceeded increased blood pressure due to amelioration of heart function.

It has been shown that expression of TGF-β1 and collagen mRNA was increased by Ang-II, and that candesartan decreased them in the heart of hypertensive rats [21, 22]. In the present study, we observed that expression of TGF-β1 and collagen-III mRNA was increased in Group-V, and these increased mRNA was suppressed by candesartan treatment in a dose-dependent manner. Thus, in our observations, taken together with the above reports suggest that Ang-II type 1 (AT1) receptor have a important role in cardiac remodeling via expression of TGF-β1 and collagen-III mRNA, and that candesartan may contribute to the inhibition of cardiac remodeling by suppressing the expression of TGF-β1 and collagen-III mRNA.

Recently, it has been reported that mechanical stress activates AT1 receptor without the involvement of Ang-II, and this activation was suppressed by candesartan but not competitive ARB [23]. Previously, Kashimura *et al.* reported that ARB TA-606 showed no significant change in the hemodynamic parameter [24]. The difference between the result of Kashimurra *et al.* with present study may be due to the characteristic of candesartan that has anchor domain which stabilizes the AT1 receptor to inactivity, resulting in inhibition of AT1 receptor by not only Ang-II but also mechanical stress.

Previously, we reported that the β-adrenoreceptor blocking agent carvedilol improved cardiac function, fibrosis area and heart weight in rats with dilated cardiomyopathy [14]. Interestingly, these changes were independent of dose. And, we observed that calcium channel antagonist amlodipine aggravated the heart failure at high dose (unpublished observation). Whereas, we observed in this study that candesartan has ameliorated the heart failure in a dose-dependent manner. These results suggest that candesartan may ameliorate the heart failure by not only hypotensive effect but also cardioprotective effect which is more eminent than other hypotensive agent.

Recently, Godsel *et al.* demonstrated that ACEI captopril prevents experimental autoimmune myocarditis [25], and we have observed that candesartan also prevented myocarditis in same animal model (unpublished ovservation). These results suggest that candesartan may prevent the inflammatory response in autoimmune myocarditis. Further studies are needed to determine whether immunological modulation for myocarditis itself could not affect the present data concerning heart failure status through the treatment with candesartan.

Conclusion, in this study, candesartan decreased myocardial fibrosis and mRNA expression of TGF-β1 and collagen-III in rats with dilated caldiomyopathy. This suggests that candesartan can be used in the treatment of various cases of heart failure.

Acknowledgments

This research was supported by grants from "the Yujin Memorial Grant," "the Ministry of Education, Science, Sports

and Culture of Japan" and "the Promotion and Mutual Aid Corporation for Private Schools of Japan."

References

1. CONSENSUS trial study group: Effects of enalapril on mortality in severe congestive heart failure: Results of the Cooperative North Scandinavian enalapril Survival Study (CONSENSUS). N Engl J Med 316: 1429–1435, 1987
2. Cohn JN, Johnson G, Ziesche S, Cobb F, Francis G, Tristani F, Smith R, Dunkman WB, Loeb H, Wong M: A comparison of enarapril with hydralazine-isosorbide dinitrate in the treatment of congestive heart failure. N Engl J Med 324: 303–310, 1991
3. SOLVD investigators: Effects of enarapril on survival in patients with reduced left ventricular ejection fractions and congestive heart failure. N Engl J Med 325: 293–302, 1991
4. Weinberg EO, Schoen FJ, George D, Kagaya Y, Douglas PS, Litwin SE, Schunkert H, Benedict CR, Lorell BH: Angiotensin-converting enzyme inhibition prolongs survival and modifies the transition to heart failure in rats with pressure overload hypertrophy due to ascending aortic stenosis. Circulation 90: 1410–1422, 1994
5. Litwin SE, Katz SE, Weinberg EO, Lorell BH, Aurigemma GP, Douglas PS: Serial echocardiographic-Doppler assessment of left ventricular geometry and function in rats with pressure-overload hypertrophy. Chronic angiotensin-converting enzyme inhibition attenuates the transition to heart failure. Circulation 91: 2642–2654, 1995
6. Weber KT, Brilla CG: Pathological hypertrophy and cardiac interstitium. Fibrosis and renin-angiotensin-aldosterone system. Circulation 83: 1849–1865, 1991
7. Swynghedauw B: Molecular mechanisms of myocardial remodeling. Physiol Rev 79: 215–262, 1999
8. Powell JS, Clozel JP, Muller RK, Kuhn H, Hefti F, Hosang M, Baumgartner HR: Inhibitors of angiotensin-converting enzyme prevent myointimal proliferation after vascular injury. Science 245: 186–188, 1989
9. Schelling P, Fischer H, Ganten D: Angiotensin and cell growth: A link to cardiovascular hypertrophy? J Hypertens 9: 3–15, 1991
10. Pfeffer MA, Swedbelg K, Granger CB, Held P, McMurray JJ, Michelson EL, Olofsson B, Ostergren J, Yusuf S; CHARM Investigators and Committees: Effects of candesartan on mortality and morbidity in patients with chronic heart failure: The CHARM-Overall programme. Lancet 362: 759–766, 2003
11. McMurray JJ, Ostergren J, Swedberg K, Granger CB, Held P, Michelson EL, Olofsson B, Yusuf S, Pfeffer MA; CHARM Investigators and Committees: Effects of candesartan in patients with heart failure and reduced left-ventricular systolic function taking angiotensin-converting-enzyme inhibitors: the CHARM-Added trial. Lancet 362: 767–771, 2003
12. Ma M, Watanabe K, Wahed IIM, Inoue M, Sekiguchi T, Kouda T, Ohta Y, Nakazawa M, Yoshida Y, Yamamoto T, Hanawa H, Kodama M, Fuse K, Aizawa Y: Inhibition of progression of heart failure and expression of TGF-β1 mRNA in rats with heart failure by the ACE inhibitor quinapril. J Cardiovasc Pharmacol 38: S51—S54, 2001
13. Kodama M, Hanawa H, Saeki M, Hosono M, Inomata T, Suzuki K, Shibata A: Rat dilated cardiomyopathy after autoimmune giant cell myocarditis. Circ Res 75: 278–284, 1994
14. Watanabe K, Ohta Y, Nakazawa M, Higuchi H, Hasegawa G, Naito M, Fuse K, Ito M, Hirono S, Tanabe N, Hanawa H, Kato K, Kodama M, Aizawa Y: Low dose carvedilol inhibits progression of heart failure in rats with dilated cardiomyopathy. Br J Pharmacol 130: 1489–1495, 2000
15. Ohta Y, Watanabe K, Nakazawa M, Yamamoto T, Ma M, Fuse K, Ito M, Hirono S, Tanabe T, Hanawa H, Kato T, Kodama M, Aizawa Y: Carvedilol enhances atrial and brain natriuretic peptide mRNA expression and release in rat heart. J Cardiovasc Pharmacol 36(suppl 2): S19–S23, 2000
16. Chomczynski P, Sacchi N: Single-step method of mRNA by acid guanidinium thiocyanate-phenol-chloroform extraction. Anal Biochem 162: 156–159, 1987
17. Fujinaka H, Yamamoto T, Feng L, Kawasaki K, Yaoita E, Hirose S, Goto S, Wilson CB, Uchiyama M, Kihara I: Crucial role of CD8-positive lymphocytes in glomerular expression of ICAM-1 and cytokines in crescentic glomerulonephritis of WKY rats. J Immunol 158: 4978–4983, 1997
18. Granger CB, McMurray JJ, Yusuf S, Held P, Michelson EL, Olofsson B, Ostergren J, Pfeffer MA, Swedberg K; CHARM Investigators and Committees: Effects of candesartan in patients with chronic heart failure and reduced left-ventricular systolic function intolerant to angiotensin-converting-enzyme inhibitors: The CHARM-Alternative trial. Lancet 362: 772–776, 2003
19. Yusuf S, Pfeffer MA, Swedberg K, Granger CB, Held P, McMurray JJ, Michelson EL, Olofsson B, Ostergren J; CHARM Investigators and Committees: Effects of candesartan in patients with chronic heart failure and preserved left-ventricular ejection fraction: The CHARM-Preserved Trial. Lancet 362: 777–781, 2003
20. Juan W, Nakazawa M, Watanabe K, Ma M, Wahed IIM, Hasegawa G, Naito M, Yamamoto T, Fuse K, Kato K, Kodama M, Aizawa Y: Quinapril inhibits progression of heart failure and fibrosis in rats with dilated cardiomyopathy after myocarditis. Mol Cell Biochem 251: 77–82, 2003
21. Kim S, Ohta K, Hamaguchi A, Yukimura T, Miura K, Iwao H: Angiotensin II induces cardiac phenotypic modulation and remodeling in vivo in rats. Hypertension 25: 1252–1259, 1995
22. Kim S, Ohta K, Hamaguchi A, Omura T, Yukimura T, Miura K, Inada Y, Ishimura Y, Chatani F, Iwao H: Angiotensin II type I receptor antagonist inhibits the gene expression of transforming grows factor-β1 and extracellular matrix in cardiac and vascular tissues of hypertensive rats. J Pharmacol Exp Ther 273: 509–515, 1995
23. Zou Y, Akazawa H, Qin Y, Sano M, Takano H, Minamino T, Makita N, Iwanaga K, Zhu W, Kudoh S, Toko H, Tamura K, Kihara M, Nagai T, Fukamizu A, Umemura S, Iiri T, Fujita T, Komuro I: Mechanical stress activates angiotensin II type I receptor without the involvement of angiotensin II. Nat Cell Biol 6(6): 499–506, 2004
24. Kashimura T, Hayashi M, Kodama M, Nakazawa M, Abe S, Yoshida T, Tachikawa H, Hanawa H, Kato K, Watanabe K, Aizawa Y: Effects of imidapril and TA-606 on rat dilated cardiomyopathy after myocarditis. Jpn Heart J 44: 735–744, 2003
25. Godsel LM, Leon JS, Wang K, Fornek JL, Molteni A, Engman DM: Captopril prevents experimental autoimmune myocarditis. J Immunol 171: 346–352, 2003

Amiodarone Improves Cardiac Sympathetic Nerve Function to Hold Norepinephrine in the Heart, Prevents Left Ventricular Remodeling, and Improves Cardiac Function in Rat Dilated Cardiomyopathy

Hitoshi Tachikawa, MD; Makoto Kodama, MD; Kenichi Watanabe, MD, PhD; Toshihiro Takahashi, PhD; Meilei Ma, PhD; Takeshi Kashimura, MD; Masahiro Ito, MD; Satoru Hirono, MD; Yuji Okura, MD; Kiminori Kato, MD; Haruo Hanawa, MD; Yoshifusa Aizawa, MD

Background—It is unclear how amiodarone therapy exerts its effects on left ventricular remodeling and cardiac sympathetic nerve function in chronic heart failure. We investigated long-term effects of amiodarone on rat dilated cardiomyopathy after healing of cardiac myosin–induced autoimmune myocarditis.

Methods and Results—Rats were treated with oral amiodarone or vehicle for 6 weeks. We determined cardiac function, left ventricular remodeling, and cardiac sympathetic nerve function with iodine-125–labeled metaiodobenzylguanidine ([I^{125}]MIBG). Amiodarone treatment improved left ventricular pressure, central venous pressure, and rate of isovolumetric contraction and decreased ventricular weight ($P<0.005$). Expression of cytokine mRNA was unchanged; expression of atrial natriuretic peptide, collagen III, and transforming growth factor-β_1 mRNA was decreased in amiodarone-treated rats ($P<0.05$). Phenotype of myosin heavy chain was moved toward that of normal rats by amiodarone. Initial myocardial uptake of MIBG decreased by 67% ($P<0.001$) and washout rate accelerated by 221% in rats with chronic heart failure compared with normal rats. Whereas amiodarone decreased the initial uptake by 71% in normal rats, amiodarone decelerated the early washout and the late washout and improved the late myocardial distribution of MIBG in rats with chronic heart failure (257% compared with vehicle-treated rats with chronic heart failure; $P<0.01$). In proportion to MIBG distributions, cardiac tissue catecholamines were increased by amiodarone treatment.

Conclusions—Long-term amiodarone treatment prevented left ventricular remodeling and improved cardiac function in rat dilated cardiomyopathy. Long-term amiodarone treatment also restored cardiac sympathetic tone to hold norepinephrine in the heart. (***Circulation.* 2005;111:894-899.**)

Key Words: cardiomyopathy ■ antiarrhythmia agents ■ remodeling ■ nervous system, sympathetic

Sudden cardiac death and progressive deterioration of left ventricular function remain major clinical problems in the management of heart failure. β-Blockers and angiotensin-converting enzyme inhibitors improve functional status and reduce mortality in patients with heart failure. Amiodarone has already been shown to be efficacious for ventricular arrhythmia in patients with left ventricular dysfunction. The results obtained from clinical trials are controversial with regard to the efficacy of amiodarone in heart failure.[1–6] Favorable outcomes of amiodarone treatment on mortality and on left ventricular function were shown in some selected patients,[2,3] although the amount of benefit remains imprecise. Recent trials could not show additional efficacy except for decrease of heart rate, prevention of lethal arrhythmias, and improvement of cost-effectiveness.[4–6] Discordances among those results may depend on the pleiotropic actions of amiodarone. The precise mechanisms of the beneficial actions of amiodarone on chronic heart failure are still uncertain.

The specific causes of heart failure may characterize the nature of left ventricular remodeling, clinical course, and response to therapy. Rat experimental autoimmune myocarditis leads to chronic heart failure such as dilated cardiomyopathy after healing of the inflammation.[7] Amiodarone has been studied in several animal models, showing some beneficial effects,[8–10] but the manner in which amiodarone improves cardiac function or heart failure remains to be clarified. In the present study we assessed the effects of

Received June 29, 2004; revision received September 24, 2004; accepted October 6, 2004.

From the First Department of Internal Medicine (H.T., M.K., T.K., M.I., S.H., Y.O., K.K., H.H., Y.A.), Radioisotope Center (T.T.), Niigata University Graduate School of Medicine, and Department of Clinical Pharmacology, Niigata College of Pharmacy (K.W., M.M.), Niigata, Japan.

The online-only Data Supplement, which contains an additional figure, can be found with this article at http://www.circulationaha.org.

Correspondence to Hitoshi Tachikawa, MD, First Department of Internal Medicine, Niigata University Graduate School of Medicine, Asahimachi 1-754, Niigata 951-8510, Japan. E-mail TachiHH@aol.com

Circulation is available at http://www.circulationaha.org

DOI: 10.1161/01.CIR.0000155610.49706.D2

amiodarone on left ventricular remodeling and cardiac function in inflammatory cardiomyopathy.

Single-photon emission CT imaging with the use of radioiodinated metaiodobenzylguanidine (MIBG), an analogue of norepinephrine with the same affinity for the sympathetic nervous system, enables quantitative assessment of norepinephrine behavior as a result of release and reuptake at the adrenergic presynaptic site. The myocardial accumulation of MIBG and its washout rate from the heart are useful indicators to evaluate the severity of dilated cardiomyopathy and the response to therapy with β-blockers.[11-13]

The purpose of the present study is to examine the in vivo effects of amiodarone on left ventricular remodeling, cardiac hemodynamics, and cardiac sympathetic function in an animal model of inflammatory cardiomyopathy.

Methods

Experimental Animals

Male Lewis rats (aged 8 weeks) were purchased from Charles River, Japan (Yokohama, Japan) and maintained in our facilities. Experimental autoimmune myocarditis was induced by immunization with purified pig cardiac myosin as previously described.[14] Rats surviving 28 days after immunization were allocated to the study groups. We treated rats for 6 weeks until day 70 and evaluated them at day 73. The study protocol was conducted according to the guidelines on animal experimentation of our institute.

Experiment 1

First, we examined the effects of amiodarone on left ventricular remodeling and cardiac function. We designed the following groups: rats with chronic heart failure treated with very-low-dose amiodarone (5 mg/kg daily; amiodarone 5 mg group; n=8); rats with chronic heart failure treated with regular-dose amiodarone (50 mg/kg daily; amiodarone 50 mg group; n=8); rats with chronic heart failure treated with vehicle alone (methylcellulose 0.5 mL daily; CHF group; n=8); and age-matched normal control rats (NC group; n=4).

Cardiac Function Assessment

ECG (SP-98, Softron) was recorded before (at day 28) and during treatment (at day 50, 3 weeks after the start of treatment) while rats were anesthetized with ether. At day 73, rats were anesthetized with 0.5% halothane mixed with 100% oxygen, and systemic and left ventricular hemodynamic parameters were recorded as described previously.[15,16] Blood samples were obtained from the inferior vena cava to measure serum concentration of amiodarone and thyroid hormone. The ventricle was excised and weighed. The mid-ventricle was cut into 2-mm transverse slices, fixed in 10% formalin, embedded in paraffin, sectioned, and stained with the hematoxylin-eosin and Azan-Mallory methods. Myocardial fibrosis was assessed as the ratio of the fibrosis area to the whole area of the section as described previously,[16] with the use of a color image analyzer (Mac Scope, MITANI Co) by use of the differences in Azan-Mallory–stained color (blue fibrosis area as opposed to red myocardium). Cross-sectional width of cardiomyocytes was evaluated in hematoxylin-eosin–stained sections. For each section, 3 epicardial and 3 endocardial areas that displayed cross sections of cardiomyocytes were selected. In each selected area, the widths of the cardiomyocytes through the nuclei of 15 cardiomyocytes were measured with an image analyzer (Mac Scope).

mRNA Analysis

Analysis of mRNA was performed by ribonuclease (RNase) protection assay and by quantitative real-time reverse transcription–polymerase chain reaction (RT-PCR). Total myocardial RNA was extracted, electrophoresed on 1.1 mol/L formaldehyde–containing 1% agarose gels, and transferred to nylon membranes. The membranes were incubated with ^{32}P-labeled cDNA probes and analyzed on a Fuji system analyzer (Fuji Photo Film Co). The cDNA probes used were for rat atrial natriuretic peptide (r-ANP), tumor necrosis factor-α (TNF-α), and interleukin-6 (IL-6). In addition, mRNA analysis by quantitative real-time RT-PCR was performed as described elsewhere[17] with the use of each primer, r-ANP, collagen type III, transforming growth factor-β_1 (TGF-β_1), sarcoplasmic reticulum calcium ATPase, TNF-α, and α- and β-type cardiac myosin heavy chain (α-MHC and β-MHC).

Experiment 2

MIBG Accumulation and Autoradiography

A total of 65 rats were used in experiment 2. After myocarditis, dilated cardiomyopathy was induced in 34 rats and treated with 50 mg/kg daily of amiodarone (CHF+A group; n=16) or methylcellulose 0.5 mL daily (CHF group; n=18). Age-matched normal rats were treated with 50 mg/kg daily of amiodarone (N+A group; n=12) or methylcellulose 0.5 mL daily (NC group; n=19). All rats were treated by daily oral administration for 6 weeks until day 70.

At day 73, a dose of 0.8 MBq [^{125}I]MIBG was injected into the external jugular vein under anesthesia with pentobarbital sodium (10 mg/kg IP).[15,18] Rats were killed, and their hearts were quickly excised at 10, 30, and 240 minutes after [^{125}I]MIBG was injected. The apical left ventricle was quickly excised and stored in a gamma counter tube, and myocardial radioactivity was measured by a well-type scintillation counter (Aloka ARC-300). The uptake of [^{125}I]MIBG was presented as the differential absorption ratio (DAR): DAR=(radioactivity of the tissue)/(total injected radioactivity)×(body weight)/(tissue weight). We calculated cardiac washout rate (WR) from DAR for evaluating cardiac turnover of MIBG. The early WR was calculated from DAR at 10 minutes and 30 minutes: WR1=[(DAR10 minutes−DAR30 minutes)/DAR10 minutes]; the late WR was calculated from DAR at 30 minutes and 240 minutes: WR2=[(DAR30 minutes−DAR240 minutes)/DAR 30 minutes]; and total WR was calculated from DAR at 10 minutes and 240 minutes: total WR=[(DAR10 minutes−DAR240 minutes)/DAR 10 minutes]. The mid-ventricle was cut into ≈2-mm transverse slices and frozen and stored at −20°C. Sequential 60-μm–thick transverse sections were obtained, and radioactive images of the myocardium were recorded by autoradiography (BAS 5000, Fuji Film Co).

Catecholamine Concentration in Cardiac Tissue

The mid-ventricular sections harvested from rats were homogenized in 1 mL PBS with an ultrasonic homogenizer (Micro Homogenizer,

TABLE 1. Ventricle Weight, Cardiomyocyte Width, and Myocardial Fibrosis

Group	n	Plasma Amiodarone, μmol/L	Serum-Free Triiodothyronine, pmol/L	Body Weight, g	Ventricle Weight, g	Ventricle Weight/Body Weight, g/kg	Cardiomyocyte Width, μm		Fibrosis, %
							Endocardium	Epicardium	
NC	4	...	...	441.2±17.1†	1.22±0.05‡	2.27±0.09†	13.4±0.2†	13.8±0.2†	3.3±0.3†
CHF	8	ND	4.03±0.34	347.3±14.4	1.42±0.04	4.13±0.16	22.9±0.6	23.9±0.7	24.6±3.2
Amiodarone 5 mg	8	ND	4.42±0.49	349.6±13.4	1.43±0.05	4.11±0.16	22.3±1.7	23.8±2.0	27.1±4.5
Amiodarone 50 mg	8	0.938±0.015	3.51±0.15	353.7±8.5	1.16±0.06*	3.26±0.11†	18.1±1.2‡	20.1±1.6	20.2±3.1

Values are mean±SE. ND indicates not detectable.
*P<0.005, †P<0.001, ‡P<0.05 vs CHF group.

TABLE 2. Hemodynamic Parameters

	NC (n=4)	CHF (n=8)	Amiodarone 5 mg (n=8)	Amiodarone 50 mg (n=8)
Heart rate, bpm	314.4±22.6	307.2±23.2	315.7±28.0	319.9±16.6
Systolic arterial pressure, mm Hg	109.5±7.0	64.6±4.9*	89.1±8.3†	91.6±6.3‡
Mean arterial pressure, mm Hg	98.3±6.5	57.4±4.8*	83.0±7.9†	84.2±6.1‡
Left ventricular pressure, mm Hg	90.4±5.5	68.7±2.5†	79.6±8.1	85.9±5.3‡
Central venous pressure, mm Hg	1.2±0.2	5.6±1.1†	5.6±1.6	1.7±0.6‡§
Left ventricular end-diastolic pressure, mm Hg	7.6±1.6	18.9±3.5†	19.9±6.3	13.0±2.4
+dP/dt, mm Hg/s	3923±575.0	2409±252.5†	2486±371.5	3520±205.7‡§
−dP/dt, mm Hg/s	−4741±701.1	−2488±445.1†	−2192±239.6	−3169±214.0

Values are mean±SE. +dP/dt indicates rate of isovolumetric contraction; −dP/dt, rate of isovolumetric relaxation.
*$P<0.001$, †$P<0.05$ vs NC group; ‡$P<0.05$ vs CHF group; §$P<0.05$ vs amiodarone 5 mg group.

Nichion Chemical) and centrifuged at 14 000 rpm for 10 minutes at 4°C. The supernatant was used for the assay. Concentrations of epinephrine and norepinephrine in myocardial tissue were measured by high-performance liquid chromatography (PLC-725CAII, Toso Co). Concentrations of IL-6 and TNF-α in myocardial tissue were also measured by enzyme-linked immunosorbent assay with commercially available kits (Genzyme Corporation). The procedures were performed according to the manufacturer's recommendations. The total protein concentration in supernatant was measured by the Pierce bicinchoninic acid protein quantification assay (Pierce Chemical Co).

Statistical Analysis

Results are presented as mean±SEM. Statistical significance was determined by 1-way ANOVA followed by the Fisher protected least significant difference method. In all tests, statistical significance was assumed at an α value of 0.05.

Results

No rats died during the chronic phase after day 28. The RR, PR, and QRS intervals were not different among the 3 groups. The QT interval was prolonged in the amiodarone 50 mg group compared with the CHF group (100.2±2.1 versus 85.4±4.0 ms; $P<0.01$). RR interval was also prolonged in the amiodarone 50 mg group, but the difference was not significant (206.4±8.6 versus 173.0±9.1 ms). Serum concentration of amiodarone was high in the amiodarone 50 mg group but was not detectable in the amiodarone 5 mg and CHF groups. Serum concentration of free triiodothyronine was not different among the 3 groups (Table 1).

Cardiac Function and Neurohumoral Parameters

Hemodynamic parameters are shown in Table 2. In the amiodarone 50 mg group, systemic arterial pressure increased and central venous pressure was decreased compared with the CHF group. The absolute value of the rate of isovolumetric contraction was also higher in the amiodarone 50 mg group than in the CHF group.

Myocardial expression of r-ANP mRNA was lower in the amiodarone 50 mg group than in the CHF group (Table 3). Myocardial MHC phenotype changed according to deterioration of left ventricular function and improvement by therapy (Figure 1 and Table 3). In the amiodarone 50 mg group, α-MHC mRNA expression increased, β-MHC mRNA expression decreased, and the ratio of α-MHC to β-MHC increased. The amiodarone 5 mg group showed no significant changes compared with the CHF group in hemodynamic parameters except for systolic and mean arterial pressure, but the ratio of α-MHC to β-MHC increased.

TABLE 3. Myocardial Tissue mRNA Expression

	NC (n=4)	CHF (n=8)	Amiodarone 5 mg (n=8)	Amiodarone 50 mg (n=8)
Atrial natriuretic peptide, 10^6 molecules mRNA/μg of total RNA	4.1±1.4	83.8±15.1*	82.4±11.7	43.9±9.7‡‖
Sarcoplasmic reticulum calcium ATPase, 10^6 molecules mRNA/μg of total RNA	454±126	418±161	212±40	306±62
Collagen III, 10^6 molecules mRNA/μg of total RNA	39±12	494±157*	474±72	174±33‡‖
TNF-α, 10^6 molecules mRNA/μg of total RNA	0.08±0.02	0.22±0.05†	0.25±0.03	0.20±0.02
TGF-β_1, 10^6 molecules mRNA/μg of total RNA	3.4±1.0	5.2±0.7	4.1±0.2	3.0±0.3§
MHC				
α-Myosin, 10^6 molecules mRNA/μg of total RNA	439±143	85±37*	79±7	115±21
β-Myosin, 10^6 molecules mRNA/μg of total RNA	227±54	116±56	85±13	109±30
Total, 10^6 molecules mRNA/μg of total RNA	666±195	251±87†	164±19	224±50
Proportion α-myosin, %	63.5±3.5	31.4±4.8*	48.9±1.6§	52.5±3.0§
Proportion β-myosin, %	36.4±3.5	68.6±4.8*	51.0±1.6§	47.4±3.0§
α-Myosin/β-myosin	1.81±0.27	0.48±0.11*	0.96±0.06‡	1.16±0.14§

Values are mean±SE.
*$P<0.001$, †$P<0.05$ vs NC group; ‡$P<0.05$, §$P<0.005$ vs CHF group; ‖$P<0.05$ vs amiodarone 5 mg group.

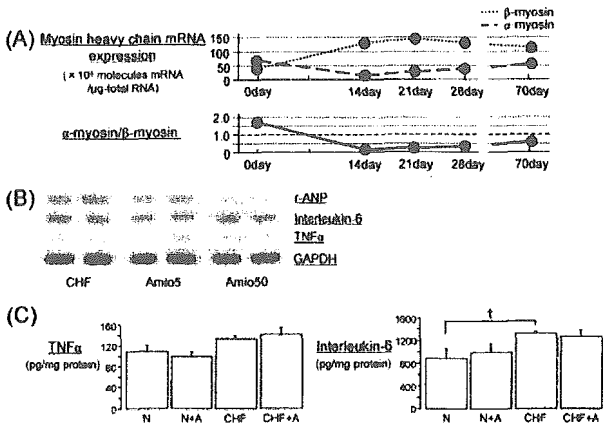

Figure 1. A, Myocardial MHC phenotype after experimental autoimmune myocarditis in rats. B, Representative bands of r-ANP, TNF-α, IL-6, and GAPDH mRNA expressions from RNase protection assay. Amio5 indicates chronic heart failure rat treated with amiodarone 5 mg/kg daily; Amio50, chronic heart failure rat treated with amiodarone 50 mg/kg daily. C, Concentrations of TNF-α and IL-6 in myocardial tissue. †$P<0.05$ vs NC rat.

Left Ventricular Remodeling and Cytokines

In the amiodarone 50 mg group, ventricular weight was lower than that in the CHF group (Table 1). Ventricular weight corrected by body weight was also smaller than that in the CHF group. Hypertrophy of cardiomyocytes was suppressed by amiodarone (Table 1 and Figure 2). The width of cardiomyocytes in the amiodarone 50 mg group was smaller than that in the CHF group. Collagen III and TGF-β_1 mRNA expression in myocardial tissue decreased in the amiodarone 50 mg group compared with values in the CHF group, whereas TNF-α and IL-6 mRNA expressions were not different among the groups. Concentrations of TNF-α and IL-6 in myocardial tissue did not change by amiodarone treatment (Table 3 and Figure 1).

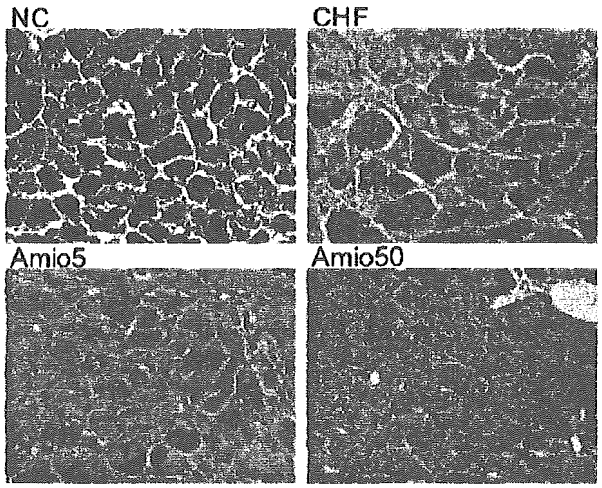

Figure 2. Myocardial histopathological changes in rats with chronic heart failure. Widespread fibrosis and various sizes of cardiomyocytes were observed in rats with chronic heart failure. Cardiomyocytes were smaller and more homogeneous in rats with heart failure treated with regular dose of amiodarone (Amio50) (hematoxylin-eosin stain; magnification ×400.) Amio5 indicates chronic heart failure rat treated with amiodarone 5 mg/kg daily; Amio50, chronic heart failure rat treated with amiodarone 50 mg/kg daily.

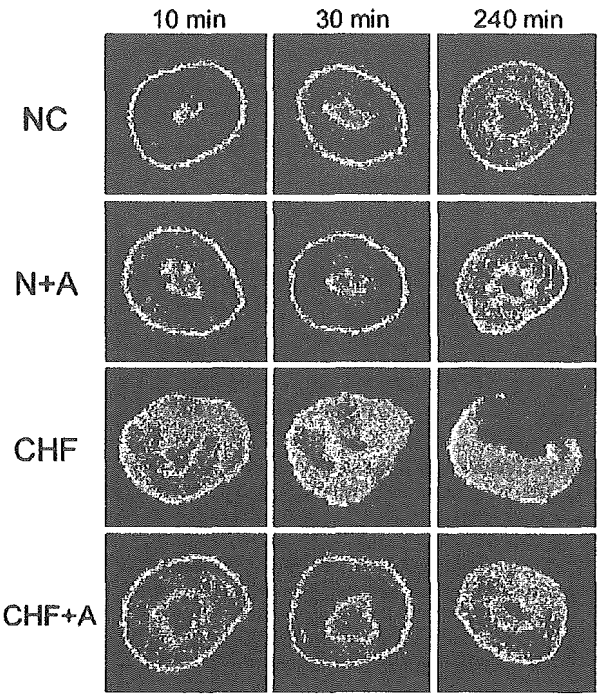

Figure 3. Autoradiographic images of ventricular MIBG distribution.

Cardiac Sympathetic Nerve Function

MIBG distribution was homogeneous in normal rats. In proportion to myocardial damage, MIBG accumulation decreased progressively and also inhomogeneously in rats with chronic heart failure (Figure 3).

The myocardial uptake of MIBG was lower in the CHF group (Figure 4 and Table 4). The early WR (WR1) was similar between the CHF and the NC groups, whereas the late WR (WR2) and total WR were markedly accelerated and the late accumulation at 240 minutes was significantly less in the CHF group compared with the NC group.

Long-term amiodarone treatment decreased the initial uptake at 10 minutes in normal rats. The early WR (WR1) was markedly decreased by amiodarone treatment in both normal rats and rats with chronic heart failure, and the accumulation at 30 minutes increased relative to the baseline at 10 minutes. The late WR (WR2) was also decreased in the CHF+A group, and the late accumulation (240 minutes) was higher than that seen in the CHF group.

Cardiac tissue catecholamines, initially at low levels in rats with chronic heart failure, increased after amiodarone treatment (Figure 4 and Table 4). Long-term amiodarone treatment increased cardiac tissue norepinephrine and epinephrine levels in normal rats and rats with chronic heart failure.

Discussion

In the present study amiodarone prevented left ventricular remodeling and improved cardiac function in rat dilated

TABLE 4. Cardiac Tissue Catecholamine Concentration, MIBG Accumulation, and WR

Group	Epinephrine, pg/g protein	Norepinephrine, pg/g protein	DAR 10 Minutes (a)	DAR 30 Minutes (b)	DAR 240 Minutes (c)	WR1 (a−b)/a, %	WR2 (b−c)/b, %	Total WR (a−c)/a, %
NC	39.7±14.3 (n=5)	3107.8±946.2 (n=5)	11.55±0.86 (n=7)	9.50±0.66 (n=4)	7.70±0.54 (n=8)	17.7	18.9	33.3
N+A	156.0±24.9* (n=5)	5878.4±522.9† (n=5)	8.30±1.06‡ (n=4)	9.41±0.46 (n=4)	6.04±0.94 (n=4)	−13.3	35.8	22.8
CHF	4.2±2.2‡ (n=5)	64.5±67.8† (n=5)	7.84±1.04* (n=7)	6.37±0.73 (n=4)	2.05±0.35§ (n=7)	18.7	67.8	73.8
CHF+A	29.8±7.4§ (n=5)	1080.9±208.2‖ (n=5)	7.52±0.89 (n=7)	7.91±0.43 (n=4)	5.27±1.29§ (n=5)	−5.1	33.4	29.9

Values are mean±SE.
*$P<0.001$, †$P<0.005$, ‡$P<0.05$ vs normal control group; §$P<0.01$, ‖$P<0.005$ vs CHF group.

cardiomyopathy after autoimmune myocarditis. Restoring the ratio of α-MHC to β-MHC (α/β) by increasing the expression level of α-MHC mRNA and decreasing that of β-MHC may contribute to improved cardiac function. A recent report showed that β-MHC mRNA decreased independent of the improvement of cardiac function in patients with dilated cardiomyopathy who were treated with a β-blocker.[19] We cannot answer whether the modulation of gene expression profiles observed in this study is caused by the direct action of amiodarone or the improvement of heart failure. Our study also showed a significant decrease of TGF-β_1 expression by amiodarone treatment, which might partially contribute to the phenotypic change of MHC. In contrast, there were no differences in the myocardial TNF-α and IL-6 levels with or without amiodarone despite persistent expression of some inflammatory cytokines. TNF-α may directly contribute to the deterioration of heart function. A clinical trial subanalysis indicated that the efficacy of amiodarone in heart failure may be partly related to inhibiting production of TNF-α.[20] Recent studies showed that amiodarone modulates the production of TNF-α and IL-6, which may attenuate myocardial injury and prevent left ventricular remodeling in human and mouse myocarditis.[10,21] Even though the drug exerted its expected biological effects, TNF-α antagonism failed to produce clinical benefits in patients with heart failure.[22] We believe that the pathogenesis of the chronic phase of this rat model is ventricular remodeling in response to diffusely scattered myocardial fibrosis.[7] Suppression of TGF-β_1 seemed to be important in preventing left ventricular remodeling by long-term amiodarone treatment.

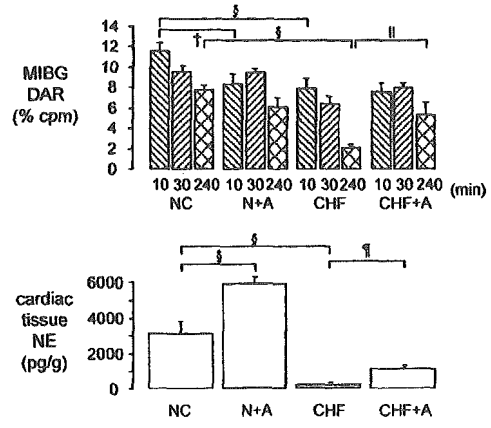

Figure 4. Cardiac norepinephrine (NE) level (bottom) and cardiac MIBG distribution represented as DAR measured by scintillation counter (top). †$P<0.05$, §$P<0.001$, ‖$P<0.01$, ¶$P<0.005$.

Our present study found a low initial uptake and a lower late accumulation of norepinephrine in rats with chronic heart failure. This faster washout may be attributed to increased norepinephrine spillover and clearance in chronic heart failure. The consequent cardiac catecholamine depletion may explain the low cardiac catecholamine levels shown in our present study. Amiodarone increased cardiac catecholamine levels to restore adrenergic order in both normal and CHF rats. MIBG WR was also decreased; these results were similar to the findings demonstrated by Kaye et al[23] that amiodarone improved cardiac sympathetic nerve function with a low cardiac norepinephrine spillover rate in patients with heart failure.

It is interesting that amiodarone shifts the peak accumulation from 10 to 30 minutes. This effect on MIBG kinetics was observed in both normal rats and CHF rats, and it is an identical effect of amiodarone. There are 2 mechanisms for the shift of the peak. One is that the initial uptake of MIBG is delayed by amiodarone. The uptake-2 system must be delayed mainly because the uptake-2 system is passive diffusion with rapid turnover, whereas the uptake-1 system is long-lasting filling into the storage vesicle.[24,25] Another mechanism is that amiodarone enhances the uptake-1 system. The uptake-1 system has a dual mechanism of reuptake and release, and the vesicular storage is mediated by a reversed neuronal reuptake mechanism that is enhanced by inhibition of the sodium-potassium adenosine triphosphatase "pump" in myocardial ischemia.[26,27] Amiodarone accelerated WR2 in the normal rats; however, the uptake may prevail and total WR may be decreased, resulting in holding norepinephrine in the heart.

Central and peripheral actions of amiodarone on cardiovascular autonomic nervous system have been reported.[28–33] The antiadrenergic effect of amiodarone is, however, different from that of β-blockers because amiodarone is noncompetitive and additive to the effects of β-blockers.[29,30] Amiodarone has various effects on sympathetic and vagal activity, such as direct Na^+ and Ca^{2+} channel–blocking properties,[31] inhibition of the muscarinic acetylcholine receptor–operated K^+ current,[32] and reserpinelike sympatholytic action.[33] These effects may depress the automaticity of sinus node and sympathetic tone. Du et al[33] observed hypotension, decreased heart rate, and depressed inotropic response of the ventricle to sympathetic activation after intravenous amiodarone admin-

istration. In our present study long-term amiodarone treatment improved the left ventricular systolic function, as shown by the increase of positive dP/dt. It is possible that holding norepinephrine in the heart and a change of cardiac myosin phenotype may contribute to enforcing cardiac contractility to improve hemodynamic parameters. However, caution is necessary when the findings of this study obtained from rats are extrapolated into clinical practice because we have not examined this aspect in humans.

In conclusion, long-term amiodarone treatment suppressed left ventricular remodeling and improved cardiac function in rat dilated cardiomyopathy after autoimmune myocarditis. In vivo assessment of cardiac sympathetic nerve function with the use of MIBG showed a lower WR and an increased late accumulation of MIBG, which would hold norepinephrine in the heart. Thus, amiodarone treatment may be beneficial in chronic heart failure.

Acknowledgments

This work was supported in part by a grant for research on specific diseases of the Ministry of Health, Labor, and Welfare.

References

1. Singh SN, Fletcher RD, Fisher SG, et al, for the Survival Trial of Antiarrhythmic Therapy in Congestive Heart Failure (STAT-CHF). Amiodarone in patients with congestive heart failure and asymptomatic ventricular arrhythmia. *N Engl J Med.* 1995;333:77–82.
2. Doval HC, Nul DR, Gambarte A, et al, for Grupo de Estudio de la Sobrevida en la Insuficiencia Cardiaca en Argentina (GESICA). Randomized trial of low-dose amiodarone in severe congestive heart failure. *Lancet.* 1994;344:493–498.
3. Boutitie F, Boissel JP, Connolly SJ, et al, and the EMIAT and CAMIAT Investigators. Amiodarone interaction with β-blockers: analysis of the merged EMIAT (European Myocardial Infarct Amiodarone Trial) and CAMIAT (Canadian Amiodarone Myocardial Infarction Trial) databases. *Circulation.* 1999;99:2268–2275.
4. Amiodarone Trials Meta-Analysis Investigators. Effect of prophylactic amiodarone on mortality after acute myocardial infarction and in congestive heart failure: meta-analysis of individual data from 6500 patients in randomized trials. *Lancet.* 1997;350:1417–1424.
5. Strickberger SA, Hummel JD, Bartlett TG, et al, for the AMIOVIRT Investigators. Amiodarone versus implantable cardioverter-defibrillator: randomized trial in patients with nonischemic dilated cardiomyopathy and asymptomatic nonsustained ventricular tachycardia: AMIOVIRT. *J Am Coll Cardiol.* 2003;41:1707–1712.
6. Moss AJ, Zareba W, Hall WJ, et al, for the Multicenter Automatic Defibrillator Implantation Trial II Investigators. Prophylactic implantation of a defibrillator in patients with myocardial infarction and reduced ejection fraction. *N Engl J Med.* 2002;346:877–883.
7. Kodama M, Hanawa H, Saeki M, et al. Rat dilated cardiomyopathy after autoimmune giant cell myocarditis. *Circ Res.* 1994;75:278–284.
8. Djandjighian L, Planchenault J, Finance O, et al. Hemodynamic and antiadrenergic effects of dronedarone and amiodarone in animals with a healed myocardial infarction. *J Cardiovasc Pharmacol.* 2000;36:376–383.
9. Silva VJD, Viana CC, Alves R, et al. Antihypertensive action of amiodarone in spontaneous hypertensive rats. *Hypertension.* 2001;38:597–601.
10. Ito H, Ono K, Nishio R, et al. Amiodarone inhibits interleukin 6 production and attributes myocardial injury induced by viral myocarditis in mice. *Cytokines.* 2002;17:197–202.
11. Rabinovitch MA, Rose CP, Rouleau JL, et al. Metaiodobenzylguanidine [131I] scintigraphy detects impaired myocardial sympathetic neuronal transport function of canine mechanical-overload heart failure. *Circ Res.* 1987;61:797–804.
12. Henderson EB, Kahn JK, Corbett JR, et al. Abnormal I-123-metaiodobenzylguanidine myocardial washout and distribution may reflect myocardial adrenergic derangement in patients with congestive cardiomyopathy. *Circulation.* 1988;78:1192–1199.
13. Wichter T, Matheja P, Eckardt L, et al. Cardiac autonomic dysfunction in Brugada syndrome. *Circulation.* 2002;105:702–706.
14. Kodama M, Matsumoto Y, Fujiwara, et al. A novel experimental model of giant cell myocarditis induced in rats by immunization with cardiac myosin fraction. *Clin Immunol Immunopathol.* 1990;57:250–262.
15. Watanabe K, Takahashi T, Nakazawa M, et al. Effect of carvedilol on cardiac function and adrenergic neural damage in rats with dilated cardiomyopathy. *J Nucl Med.* 2002;43:531–535.
16. Tachikawa H, Kodama M, Hui L, et al. Angiotensin II type 1 receptor blocker, valsartan, prevented cardiac fibrosis in rat cardiomyopathy after autoimmune myocarditis. *J Cardiovasc Pharmacol.* 2003;41(suppl 1):S105–S110.
17. Hanawa H, Abe S, Hayashi M, et al. Time course of gene expression in rat experimental autoimmune myocarditis. *Clin Sci.* 2002;103:623–632.
18. Nozawa T, Igawa A, Yoshida N, et al. Dual-tracer assessment of coupling between cardiac sympathetic neuronal function and downregulation of β-receptors during development of hypertensive heart failure of rats. *Circulation.* 1998;97:2359–2367.
19. Lowes BD, Gilbert EM, Abraham WT, et al. Myocardial gene expression in dilated cardiomyopathy treated with beta-blocking agents. *N Engl J Med.* 2002;346:1357–1365.
20. Oral H, Fisher SG, Fay WP, et al. Effects of amiodarone on tumor necrosis factor-α levels in congestive heart failure secondary to ischemic or idiopathic dilated cardiomyopathy. *Am J Cardiol.* 1999;83:388–391.
21. Matsumori A, Ono K, Nishio R, et al. Amiodarone inhibits production of tumor necrosis factor-α by human mononuclear cells. *Circulation.* 1997;96:1386–1389.
22. Chung ES, Packer M, Lo KH, et al, for the Anti-TNF Therapy Against Congestive Heart Failure Investigators. Randomized, double-blind, placebo-controlled, pilot trial of infliximab, a chimeric monoclonal antibody to tumor necrosis factor-alpha, in patients with moderate-to-severe heart failure: results of the anti-TNF Therapy Against Congestive Heart Failure (ATTACH) trial. *Circulation.* 2003;107:3133–3140.
23. Kaye DM, Dart AM, Jennings GL, et al. Antiadrenergic effects of chronic amiodarone therapy in human heart failure. *J Am Coll Cardiol.* 1999;33:1553–1559.
24. Eisenhofer G, Ropchak TG, Kopin IJ, et al. Release, metabolism and intraneuronal disposition of exogenous, endogenous and newly synthesized norepinephrine in the rat vas deferens. *J Pharmacol Exp Ther.* 1988;245:81–88.
25. Nakajo M, Shimabukuro K, Yoshimura H, et al. Iodine-131 metaiodobenzylguanidine intra-and extravesicular accumulation in the rat heart. *J Nucl Med.* 1986;27:84–89.
26. Kranzhofer R, Haass M, Kurz T, et al. Effect of digitalis glycosides on norepinephrine release in the heart: dual mechanism of action. *Circ Res.* 1991;68:1628–1637.
27. Lameris TW, Zeeuw S, Alberts G, et al. Time course and mechanism of myocardial catecholamine release during transient ischemia in vivo. *Circulation.* 2000;101:2645–2650.
28. Dias Da Silva VJ, Gnecchi-Ruscone T, Lavelli B, et al. Opposite effects of IV amiodarone on cardiovascular vagal and sympathetic efferent activities in rats. *Am J Physiol.* 2002;283:R543–R548.
29. Charlier R. Cardiac actions in the dog of a new antagonist of adrenergic excitation which dose not produce competitive blockade of adrenoceptors. *Br J Pharmacol.* 1970;39:668–674.
30. Drvata V, Haggblad J, Blange I, et al. The effect of amiodarone on the β-adrenergic receptor is due to a downregulation of receptor protein and not to a receptor-ligand interaction. *Biochem Biophys Res Commun.* 1999;255:515–520.
31. Mitchell LB, Wyse G, Gillis AM, et al. Electropharmacology of amiodarone therapy initiation. *Circulation.* 1989;80:34–42.
32. Watanabe Y, Hara Y, Tamagawa M, et al. Inhibitory effect of amiodarone on the muscarinic acetylcholine receptor–operated potassium current in guinea pig atrial cells. *J Pharmacol Exp Ther.* 1996;279:617–624.
33. Du XJ, Esler MD, Dart AM. Sympatholytic action of intravenous amiodarone in the rat heart. *Circulation.* 1995;91:462–470.

ELSEVIER

The European Journal of Heart Failure 7 (2005) 109–112

The European Journal of Heart Failure

www.elsevier.com/locate/heafai

Short report

Short-term prognostic value of initial serum levels of interleukin-10 in patients with acute myocarditis

Koichi Fuse*, Makoto Kodama, Yuji Okura, Masahiro Ito, Kiminori Kato, Haruo Hanawa, Yoshifusa Aizawa

Division of Cardiology, Niigata University Graduate School of Medical and Dental Sciences, 1-754 Asahimachi-dori, Niigata City 951-8510, Japan

Received 5 October 2003; received in revised form 20 January 2004; accepted 20 March 2004
Available online 25 May 2004

Abstract

The disease course of acute myocarditis has a wide spectrum and the predictors of the prognosis in patients with acute myocarditis have not yet been established. In the pathogenesis of myocarditis, the cytokine environment is important. In this study, we examined the predictive values of serum levels of interleukin-10 (IL-10) and IL-12 in the short-term prognosis of patients with acute myocarditis. Twenty-four consecutive patients who had been diagnosed as having acute active myocarditis were analyzed and monitored for 2 months. The patients with myocarditis were divided into the survival group (n=16) and the non-survival group (n=8). Initial serum levels of IL-10 (P=0.0015) and IL-12 (P=0.012) in the non-survival group were significantly higher than those of the survival group, and there was a significant correlation between IL-10 and IL-12 levels (P<0.0001). The univariate analyses showed that increased serum levels of IL-10 (hazard ratio 1.041, P=0.0004) and IL-12 (hazard ratio 1.128, P=0.0346) were significant predictors of mortality. In the Kaplan–Meier analysis, high levels of IL-10 (≥7.0 pg/ml) (P=0.0239) strongly predicted high mortality. In conclusion, the elevation in serum IL-10 levels at the initial phase appeared to predict poor short-term prognosis in patients with acute myocarditis.

Keywords: Myocarditis; Prognosis; Interleukin-10; Interleukin-12; Th1/Th2

1. Background

The disease course of acute myocarditis has a wide spectrum and it is difficult to predict the prognosis [1–6]. Recently, it has been reported that cytokine environment, especially helper T type 1 (Th1) and helper T type 2 (Th2) balance is important in the pathogenesis of myocarditis [7–10]. We also reported that Th1/Th2 balance of peripheral lymphocytes reflected the disease activity in a patient with acute myocarditis [11]. It is important that the estimation of the disease activity of acute myocarditis, which is on going stage or healing stage at the initial stage, when predicting a prognosis and performing suitable treatment.

2. Aims

In this study, we measured initial serum levels of Interleukin-10 (IL-10), which is anti-inflammatory Th2 cytokine, and IL-12, which develops the precursor Th cells to Th1 cells and inhibits the differentiation of Th2 cells, from the patients with histopathology-proven acute myocarditis and investigated the predictive values in the short-term outcome.

3. Methods

Samples were obtained from 24 patients with biopsy or autopsy-proven active myocarditis (Dallas criteria).

* Corresponding author. *Present address*: Toronto General Hospital, 3R-408 Max Bell Research Centre, 101 College Street, Toronto, Ontario, Canada M5G1L7. Tel.: +1-416-340-3705; fax: +1-416-595-9592.
E-mail address: fuse@kd6.so-net.ne.jp (K. Fuse).

1388-9842/$ - see front matter © 2004 European Society of Cardiology. Published by Elsevier B.V. All rights reserved.
doi:10.1016/j.ejheart.2004.03.006

Table 1
Comparison of characteristics, hemodynamic data and serum biochemical markers at the time of hospitalization

	Suvivors (n=16)	Non-survivors (n=8)	P
Age (years)	47.9±4.1	51.1±7.5	NS
Sex (M/F)	12/4	5/3	NS
Days from onset until sampling (days)	7.2±2.3	7.5±2.1	NS
Systolic blood pressure (mmHg)	97.5±4.4	83.8±4.6	NS
CI (l/min/m^2)	2.4±0.2	2.0±0.3	NS
PCWP (mmHg)	18±1	22±2	NS
CPK (IU/l)	779±249	1341±415	NS
CRP (mg/dl)	6.5±2.0	6.5±2.2	NS
IL-10 (pg/ml)	6.8±1.1	38.6±11.4	0.0015
IL-12 (pg/ml)	5.8±0.9	49.2±24.9	0.0120

CI, cardiac index; PCWP, pulmonary capillary wedge pressure, CPK, creatine phosphokinase; CRP, C-reactive protein; IL-10, interleukin-10; IL-12, interleukin-12.

These patients included 17 men and seven women ranging from 15 to 70 years (mean, 49±4 years) and were divided into the survival group (those who could be discharged from the hospital) and the non-survival group (those who died during hospitalization). Hemodynamic study was performed in all patients at the time of hospitalization and nine patients were treated with percutaneous cardiopulmonary support (PCPS). Each sample was collected at the time of hospitalization and was frozen at −80 °C. Serum levels of IL-10 and IL-12 were determined by enzyme-linked immunosorbent assay kits (Biosourse International, CA, USA). Informed consent was obtained from all patients and the protocol was approved by the local ethics committee on clinical research of our institution.

Statistical comparisons of parameters between both groups were analyzed by the Mann–Whitney's U-test. Univariate Cox regression analyses were used to analyze survival time until death. Correlation was investigated by means of the Spearman's rank correlation method. The Kaplan–Meier analysis was performed on the cumulative rates of survival in patients with acute myocarditis stratified into two groups on the basis of the increased serum levels of IL-10 and IL-12 (≥ or <7.0 pg/ml and ≥ or <4.0 pg/ml, respectively). The differences between survival curves were analyzed by the log-rank test. The values are represented as mean±standard error of mean (S.E.M.). Statistical significance was accepted at P<0.05.

4. Results

All patients were followed up until 60 days from the onset of myocarditis. Eight patients died of cardiac causes during the follow-up period (mean, 28±7 days; range, 11–59 days). Age, sex, systolic blood pressure, cardiac index (CI), pulmonary capillary wedge pressure (PCWP) and days from onset until blood sampling were not significantly different between survivors and non-survivors. However, hypotension and elevation of PCWP had a trend toward worse prognosis. Creatine phosphokinase (CPK) and C-reactive protein (CRP), which are important biochemical laboratory markers at the time of admission, were also not significantly different between both groups. Serum levels of IL-10 and IL-12 in the non-survival group (38.6±11.4 pg/ml and 49.2±24.9 pg/ml, respectively) were significantly increased compared with those of the survival group (6.8±1.1 pg/ml and 5.8±0.9 pg/ml, respectively) (Table 1). Univariate analyses showed that high IL-10 (P=0.0004) and IL-12 (P=0.0346) levels were significant predictors of mortality (Table 2). In the Kaplan–Meier analysis, patients with high IL-10 levels (≥7.0 pg/ml) had a significantly higher mortality rate than those with low IL-10 levels (<7.0 pg/ml) (Fig. 1a). However, there was no significant difference between patients with high IL-12 levels (≥4.0 pg/ml) and those with low IL-12 levels (<4.0 pg/ml) (Fig. 1b). In addition, we found a significant correlation between serum levels of IL-10 and IL-12 (R=0.78, P<0.0001) (Fig. 2).

Table 2
Univariate analyses of predictors of mortality in 24 patients with acute myocarditis

	Hazard ratio	95% confidence interval	P
Systolic blood pressure (mmHg)	0.955	0.915–0.997	0.0541
CI (l/min/m^2)	0.468	0.154–1.418	0.1796
PCWP (mmHg)	1.201	1.000–1.441	0.0512
CPK (IU/l)	1.000	1.000–1.001	0.1558
CRP (mg/dl)	0.995	0.906–1.094	0.9226
IL-10 (pg/ml)	1.041	1.018–1.064	0.0004
IL-12 (pg/ml)	1.128	1.009–1.261	0.0346

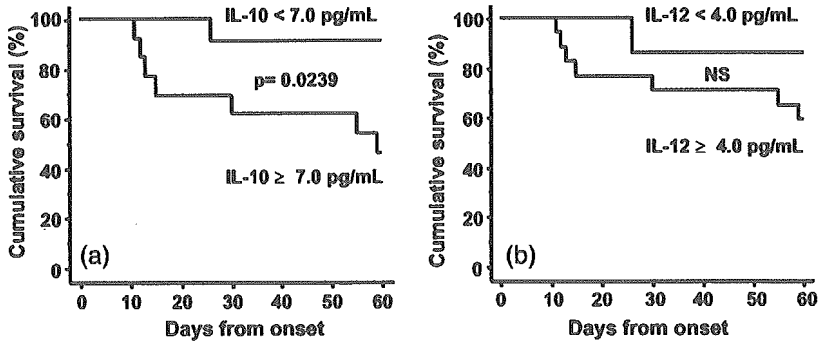

Fig. 1. Kaplan–Meier analysis of cumulative rates of survival in 24 patients with acute myocarditis stratified into two groups on basis of increased interleukin-10 (IL-10) levels (≥7.0 pg/ml or <7.0 pg/ml) (a) and IL-12 levels (≥4.0 pg/ml or <4.0 pg/ml) (b).

However, there was no significant correlation between IL-10 or IL-12 levels and systolic blood pressure, CI, PCWP, CPK or CRP levels (data were not shown).

5. Conclusions

We measured serum levels of IL-10 and IL-12 in 24 patients with acute myocarditis. IL-10 and IL-12 levels significantly increased in the non-survival group, and a high IL-10 level was shown to be a significant short-term predictor.

We focused on IL-10 and IL-12, which are both important to the evaluation of the cytokine environment in the pathogenesis of myocarditis. Previous reports have suggested the therapeutic effect of IL-10 [10,12] and IL-12 [13] in experimental myocarditis models. Meanwhile, cardiac myosin and specific T-lymphocytes can induce experimental autoimmune myocarditis when cultured with IL-12 [14]. We hypothesized that the high levels of Th1 cytokine relate to the mortality and high levels of Th2 cytokine causing a spontaneous remission. However, unexpectedly the high levels of IL-10 related to the mortality in our study. On the other hand, some studies have suggested that vigorous initial immune responses have a long-term beneficial effect in patients with myocarditis [2,15]. In human myocarditis, the duration from viral infection until onset of cardiac symptoms and the timing of the shift from Th1 dominance to Th2 dominance are still not clear. The elevated serum IL-10 levels may possibly reflect the initial amount of virus in acute myocarditis. Furthermore, exogenous delivery of IL-10 may be useful especially in the patients with myocarditis that show high levels of IL-10.

The limitations of this study are the small number of patients, and the lack of multivariate analyses. We also need to perform multi-point analyses. Despite those limitations, our study suggests that elevation of initial serum IL-10 levels appeared to be a good serological marker to predict the short-term prognosis in acute myocarditis.

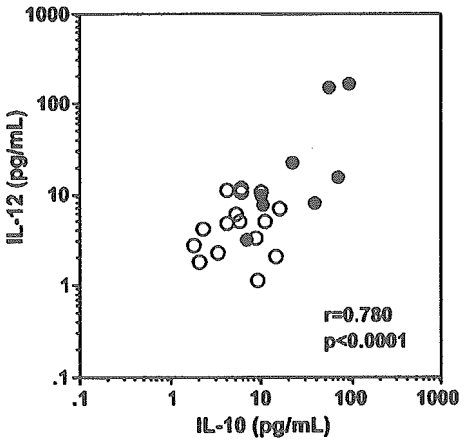

Fig. 2. Relationship between serum level of IL-10 and that of IL-12. There is a significant correlation between serum levels of IL-10 and IL-12 (R=0.78, P<0.0001). ○, Survivors; ●, Non-survivors.

References

[1] Dec GW Jr, Palacios IF, Fallon JT, et al. Active myocarditis in the spectrum of acute dilated cardiomyopathies: clinical features, histologic correlates and clinical outcome. N Engl J Med 1985;312:885–90.

[2] Mason JW, O'Connell JB, Herskowitz A, et al. A clinical trial of immunosuppressive therapy for myocarditis: the myocarditis treatment trial investigators. N Engl J Med 1995;333:269–75.

[3] McCarthy 3rd RE, Boehmer JP, Hruban RH, et al. Long-term outcome of fulminant myocarditis as compared with acute (non-fulminant) myocarditis. N Engl J Med 2000;342:690–5.

[4] Fuse K, Kodama M, Okura Y, et al. Predictors of disease course in patients with acute myocarditis. Circulation 2000;102:2829–35.

[5] Kodama M, Oda H, Okabe M, Aizawa Y, Izumi T. Early and long-term mortality of the clinical subtypes of myocarditis. Jpn Circ J 2001;65:961–4.

[6] Aoyama N, Izumi T, Hiramori K, et al. Japanese Investigators of Fulminant Myocarditis. National survey of fulminant myocarditis in Japan: therapeutic guidelines and long-term prognosis of using percutaneous cardiopulmonary support for fulminant myocarditis (special report from a scientific committee). Circ J 2002;66:133–44.

[7] Okura Y, Yamamoto T, Goto S, et al. Characterization of cytokine and iNOS mRNA expression in situ during the course of experimental autoimmune myocarditis in rats. J Mol Cell Cardiol 1997;29:491–502.

[8] Seko Y, Takahashi N, Yagita H, Okumura K, Yazaki Y. Expression of cytokine mRNAs in murine hearts with acute myocarditis caused by coxsackievirus B3. J Pathol 1997;183:105–8.
[9] Nakano A, Matsumori A, Kawamoto S, et al. Cytokine gene therapy for myocarditis by in vivo electroporation. Hum Gene Ther 2001;12: 1289–97.
[10] Watanabe K, Nakazawa M, Fuse K, et al. Protection against autoimmune myocarditis by gene transfer of interleukin-10 by electroporation. Circulation 2001;104:1098–100.
[11] Fuse K, Kodama M, Aizawa Y, et al. Th1/Th2 balance alteration in the clinical course of a patient with acute viral myocarditis. Jpn Circ J 2001;65:1082–4.
[12] Nishio R, Matsumori A, Shioi T, Ishida H, Sasayama S. Treatment of experimental viral myocarditis with interleukin-10. Circulation 1999;100:1102–8.
[13] Shioi T, Matsumori A, Nishio R, Ono K, Kakio T, Sasayama S. Protective role of interleukin-12 in viral myocarditis. J Mol Cell Cardiol 1997;29:2327–34.
[14] Okura Y, Takeda K, Honda S, et al. Rocombinant murine interleukin-12 facilitates induction of cardiac myosin-specific type 1 helper T cells in rats. Circ Res 1988;82:1035–42.
[15] McNamara DM, Holubkov R, Starling RC, et al. Controlled trial of intravenous immune globulin in recent-onset dilated cardiomyopathy. Circulation 2001;103:2254–9.

Prevention of Experimental Autoimmune Myocarditis by Hydrodynamics-Based Naked Plasmid DNA Encoding CTLA4-Ig Gene Delivery

SATORU ABE, MD,[1] HARUO HANAWA, MD,[1] MANABU HAYASHI, MD,[1] TSUYOSHI YOSHIDA, MD,[1] SATORU KOMURA, MD,[1] RITSUO WATANABE, MD,[1] HUI LIE, MD,[1] HE CHANG, MD,[1] KIMINORI KATO, MD,[1] MAKOTO KODAMA, MD,[1] HIROKI MARUYAMA, MD,[2] MIKIO NAKAZAWA, PhD,[3] JUNICHI MIYAZAKI, MD,[4] AND YOSHIFUSA AIZAWA, MD[1]

Niigata, Japan; Osaka, Japan

ABSTRACT

Background: Rat experimental autoimmune myocarditis (EAM) is a T cell–mediated disease that resembled the giant cell myocarditis seen in humans. Soluble CTLA4 improves some autoimmune diseases by blocking costimulatory signals on T cell. We investigated the effect of hydrodynamics-based naked plasmid DNA encoding CTLA4-immunoglobulin (Ig) gene delivery.

Methods and Results: Lewis rats were immunized with cardiac myosin and treated with hydrodynamic-based transfection, namely a rapid tail vein injection of a large volume of pCAGGS encoding CTLA4-Ig chimera solution on Day 0. The vector-derived CTLA4-Ig mRNA expressions were mainly detected in the liver and plasma CTLA4-Ig protein levels were maintained at about 2 μg/mL during the experiment period. On Day 17, the ratio of heart to body weight, the amount of mRNA of atrial natriuretic peptide, and the inflammatory areas in CTLA4 group were significantly lower than in the control group treated with empty plasmid. Maximum rate of intraventricular pressure rise and decline (dP/dT), minimum dP/dT, left ventricular end-diastolic pressure, and central venous pressure improved significantly after treatment with CTLA4-Ig. On Day 14, expressions of IL-2 in popliteal lymph nodes in the CTLA4-Ig group were significantly lower than in the control group.

Conclusion: Hydrodynamics-based transfection of plasmid encoding CTLA4-Ig chimera dramatically prevented EAM.

Key Words: Gene therapy, Dilated cardiomyopathy, Cytokine, pCAGGS.

We have shown previously that experimental autoimmune myocarditis (EAM), induced in the rat, is a T cell–mediated disease that resembled the giant cell myocarditis seen in humans, and that long-term administration of anti-αβT-cell receptor (TCR) antibody prevented the progression of EAM.[1-3] T cells recognize peptide–major histocompatibility complex complexes on antigen-presenting cells by TCR.[4] Then, costimulatory molecules—for example, CD28, CD4, or CD8 on T cells and CD80 (B7-1), CD86 (B7-2), or ICAM-1 on antigen-presenting cells—play important roles to enhance adhesion of T cells to antigen-presenting cells and transduce a costimulatory signal.[5] In particular, engagement of the CD28 molecule with its ligand B7 provides an essential costimulatory signal without which full activation of T cells cannot occur.[6] Exposure of T-cell clones to antigen complexes with major histocompatibility complex through TCR in the absence of the costimulatory signal induces a state of clonal anergy.[7] CTLA-4 is 44kD protein similar to CD28, and CTLA-4 exhibits about 20 times' greater binding affinity for B7 than does CD28.[8] Therefore, CTLA4-immunoglobulin (Ig) chimera protein can strongly inhibit the engagement of the CD28 with B7.[9] Matsui et al have reported that adenovirus vectors containing CTLA4-Ig improved the pathologic findings in the hearts of EAM subjects through their ability to block T-cell costimulatory signals.[10] However, adenoviruses are thought to cause viral myocarditis and adenovirus vectors themselves may influence the immunologic

From the [1]Division of Cardiology; [2]Division of Clinical Nephrology and Rheumatology, Niigata University Graduate School of Medical and Dental Science, and [3]Department of Medical Technology, School of Health Science, Niigata University School of Medicine, Niigata, Japan; [4]Division of Stem Cell Regulation, Osaka University Graduate School of Medical Science, Osaka, Japan.

Manuscript received May 24, 2004; revised manuscript received February 10, 2005; revised manuscript accepted April 8, 2005.

Reprint request: Satoru Abe, MD, First Department of Internal Medicine, Niigata University School of Medicine, Asahi-machi 1-754, Niigata, 951-8510, Japan.

Supported in part by grants for scientific research from the Ministry of Education, Science, and Culture of Japan (No. 12670653).

1071-9164/$ - see front matter

doi:10.1016/j.cardfail.2005.04.005

mechanism and cardiac function on EAM.[11,12] Moreover, tragic death by devastating inflammatory reaction to the adenoviral vector in a clinical trial for ornithine transcarbamylase deficiency was reported.[13] Therefore, adenoviruses are difficult to use for myocarditis treatment clinically. On the other hand, gene transfer by a naked plasmid vector is easier and safer than a virus vector and does not generally cause infection.[14,15] Nevertheless, a shortcoming of gene transfer by plasmid was the inability to express transgene adequately. However, it has recently been reported that hydrodynamics-based gene delivery by naked plasmid vector, namely a rapid tail vein injection of a large volume of plasmid DNA solution, could induce a sustained high-level of the encoded protein.[16–18] The serum levels of the relevant proteins acquired by this novel transfer method were high enough to suggest that it had potential as a strategy for gene therapy.[17,18] The vector-derived mRNA expression was mainly detected in the hepatocytes[17,18] and only the encoded protein was secreted. This, together with the fact that no immunologic reaction occurs, is thought to allow the role of the protein to be evaluated alone. Furthermore, modified hydrodynamics-based gene delivery by naked plasmid vector—for example, retrograde hepatic or coronary venous delivery—may be clinical gene therapy method in the future.[19] In the study discussed here, we report the effects of hydrodynamics-based naked plasmid DNA encoding CTLA4-Ig gene delivery on preventing the development of EAM in rats. CTLA4-Ig protects rats from development of EAM as evidenced by a significant reduction of the histologic cardiac cellular infiltrate and improvement in the hemodynamic status.

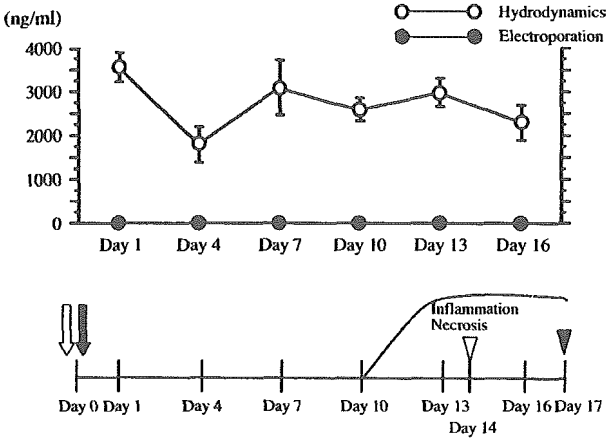

Fig. 1. Plasma rat CTLA4-Ig-Glu-tag protein levels after hydrodynamics-based gene delivery (open circle), namely a rapid tail vein injection of a large volume of pCAGGS-rat CTLA4-Ig-Glu-tag or intramuscular gene delivery (closed circle) into the tibialis anterior muscles by electroporation. Each bar represents mean ± SEM. Open arrow, immunization; solid arrow, gene transfer; open arrow head, evaluation of mRNA in popliteal lymph node; solid arrow head, physiologic and histologic evaluation.

Methods

Preparation of EAM

Male Lewis rats were purchased from Charles River Japan Inc. (Atsugi, Japan). They were maintained in our animal facilities until 8 weeks of age. Whole cardiac myosin as antigen was prepared from the ventricular muscle of porcine hearts as previously described.[1] It was dissolved in a solution of 0.3 mol/L KCl at a concentration of 10 mg/mL and emulsified with an equal volume of complete Freund's adjuvant supplemented with 10 mg/mL of *Mycobacterium tuberculosis* H37RA (Difco, Detroit, MI). On Day 0, each rat received a single immunization at two subcutaneous sites on the foot, with a total of 0.2 mL of the emulsified preparation (Fig. 1). Throughout the study, all animals were treated in accordance with our institute's guidelines for animal experiments.

Plasmid DNA for Gene Transfer

To create plasmids for plasma concentration analysis, we first constructed a plasmid pCAGGS-Ig-glucagon Tag (Glu-tag) with SwaI and NotI restriction sites using polymerase chain reaction (PCR).[20] The first PCR products were amplified from rat spleen cDNA using KOD Plus DNA polymerase (TOYOBO, Osaka, Japan) and the primers (5′-gaGAATTCATTTAAATgagaGCGGCCGCcgtgcccagaaactgtg-3′ with SwaI and NotI restriction sites and 5′-tcaaccactgcacaaaatcttgggctttacccggagagtgggagagact-3′) (uppercase letters indicate restriction enzyme sites). The final PCR product inserts were then amplified from the diluted products of the first PCR reaction with the primers (5′-gaGAATTCATTTAAATgagaGCGGCCGCcgtgcccagaaactgtg-3′ with SwaI and NotI restriction sites and 5′-gagagagaGAATTCtcaggtattcatcaaccactgcacaaaatcttgggc-3′). These products were inserted into the pCAGGS vector using EcoRI sites. *Escherichia coli* JM109 competent cells were then transformed and recombinant plasmids were isolated using a Quantum Prep Plasmid Maxiprep kit (Bio-Rad Laboratories, Hercules, CA). Next, to construct the pCAGGS-rat CTLA4-Ig-Glu-tag, rat CTLA4 cDNAs were amplified from phytohemagglutinin-stimulated splenocyte cDNA using the primers (5′-gaGAATTCATTTAAATggcttgtcttggactccagagg-3′ and 5′- gcagcatcGCGGCCGCgtctgaatctgggcatggttctgg-3′) and then inserted into the pCAGGS-Ig-Glu-tag using SwaI and NotI sites. The recombinant plasmids were isolated as described previously.

In the next stage, we constructed a plasmid pCAGGS-CTLA4-Ig for EAM treatment. The PCR products amplified from rat spleen cDNA using the primers (5′-gaGAATTCATTTAAATgagaGCGGCCGCcgtgcccagaaactgtg-3′ with SwaI and NotI restriction sites and 5′-gagagagaGAATTCactctggggtcatttacccggagagtgggag-3′) as described previously were inserted into pCAGGS vector using EcoRI sites (pCAGGS-rat Ig). *E. coli* JM109 competent cells were then transformed and recombinant plasmids were isolated as above. To construct the pCAGGS-CTLA4-Ig, rat CTLA4 cDNAs were amplified as described previously and then inserted into pCAGGS-rat Ig using SwaI and NotI sites.

Gene Transfer of Plasmid DNA

The effect of CTLA4-Ig on EAM was evaluated using previously published methods on Day 17 as follows. EAM rats were rapidly injected into tail vein on Day 0 either plasmid DNA pCAGGS-CTLA4-Ig (n = 9), or empty plasmid as a control (n = 9) at a dose of 800 μg per rat, in a volume of 20 mL (approximately 80 mL/kg body weight) within 10 seconds (Fig. 1). To evaluate the mechanism

of CTLA4-Ig effect, EAM rats prepared by the previously mentioned method, pCAGGS-CTLA4-Ig (n = 6) or empty plasmid as a control (n = 6). EAM rats were sacrificed on Day 14 and popliteal lymph nodes were taken. In addition, to measure the serum concentration of the protein, normal rats were injected with pCAGGS-rat CTLA4-Ig-Glu-tag as described previously (n = 3) (Fig. 1). We compared this with a rapid tail vein injection of a large volume and a injection into the tibialis anterior muscles by electroporation.[21] Rats (n = 4) were anesthetized with diethyl ether and injected as follows. Aliquots of 100 μL of plasmid DNA (pCAGGS-rat CTLA4-Ig-Glu-tag) at 2 μg/μL in phosphate-buffered saline were injected 4 times (total amount of DNA was 800 μg per rat) into the bilateral tibialis anterior muscles using a disposable insulin syringe with a 27-gauge needle. A pair of electrode needles with a gap of 5 mm was inserted into the muscle to a depth of 5 mm to encompass the DNA injection sites, and electrical pulses were delivered 4 times at 100 V using an electrical pulse generator (Electro Porator CUY21; TR Tech, Tokyo, Japan). To evaluate the organs expressing vector-derived CTLA4-Ig mRNA, normal rats (n = 3) were rapidly injected in the tail vein with plasmid DNA pCAGGS-CTLA4-Ig-Glu-tag.

Plasma Chimeric Protein Measurement

Blood samples were taken Days 1, 4, 10, 13, and 16 after hydrodynamics-based gene transfection or an injection into the tibialis anterior muscles by electroporation. Glucagon concentrations were measured using a glucagon radioimmunoassay Kit (Daiichi Radioisotope Labs, Tokyo, Japan).[22] Chimeric protein concentrations were calculated using the following formula: (chimeric protein concentration) = (actually measured glucagon concentration) × (chimeric protein molecular weight)/(whole glucagon molecular weight).[20]

Hemodynamic Study

On Day 17, for the surgical procedure to measure the hemodynamic parameters, rats were anesthetized initially with 2% isoflurane in oxygen and then the concentration was reduced to 0.5% to minimize the hemodynamic effect. Mean arterial pressure was recorded through a catheter introduced into the right femoral artery. Central venous pressure was recorded through a catheter introduced into the confluence of the vena cava with the right jugular vein. A catheter-tip transducer was inserted into the left ventricle from the right carotid artery to measure the peak left ventricular pressure and left ventricular end-diastolic pressure. The rate of intraventricular pressure rise and decline (±dP/dT) was measured with a differential amplifier. Heart rate was calculated from electrocardiograms. All hemodynamic parameters were recorded on a thermostylus recorder after a stabilizing period of 10 minutes.

Histopathology

After the hemodynamic study, a blood sample was obtained from the inferior vena cava. On Day 17 the heart was removed and cleaned of the surrounding tissues and atrium. The heart weight (HW) was measured and the ratio of HW to body weight (HW/BW) was calculated. For the histologic evaluation, the hearts were sectioned at three levels, and the middle one of the ventricles was fixed in 10% formalin. Paraffin-embedded tissues were cut and stained with hematoxylin-eosin and Azan-Mallory. In the biventricular cardiac cross-section, the ratio of inflammatory area was computed by digital image processor software, Lumina Vision and Mac SCOPE (Mitani Co., Maruoka, Fukui, Japan) by means of the differences in color. The results were presented as the ratio of the inflammatory area to the whole biventricular section.

Quantitative Reverse Transcription-Polymerase Chain Reaction

Total RNA was isolated from one third (apex side) of the rat's ventricle on Day 17 using Trizol (Life Technologies, Tokyo, Japan). cDNA was synthesized from 5 μg of total RNA with random primers. Construction of the plasmid with rat atrial natriuretic peptide (ANP) cDNA as a standard sample for quantitative reverse transcription-polymerase chain reaction for ANP was as previously described.[23] Briefly, to construct the standard plasmid, cDNAs of ANP were amplified using the primers (5′-atggatttcaagaacctgctagac-3′, 5′-gctccaatcctgtcaatcctac-3′) from rat heart cDNA. The amplified cDNAs were directly inserted into the pGEM-T vector and the recombinant plasmids were purified. cDNA and diluted plasmid were amplified with the same primer used for making the plasmid and LightCycler-FastStart DNA Master SYBR Green I (Roche, Indianapolis, IN) by LightCycler. The absolute copy numbers (molecules mRNA/μg of total RNA) of all the samples were calculated by the LightCycler software using this plasmid standard curve. To evaluate the mechanism of CTLA4-Ig, total RNA was isolated from popliteal lymph nodes of EAM on Day 14 and expressions of IL-2 and γ-actin mRNA were similarly examined using the primers (IL-2, 5′-ctgagagggatcgataattacaaga-3′, 5′-attggcactcaaatttgttttcag-3′; γ-actin, 5′-agccttccttcctgggcatggagt-3′, 5′-tggaggggccctgactcgtcatact-3′).

Vector-Derived CTLA4-Ig mRNA Expression

Total RNA was isolated from livers, kidneys, hearts, lungs, and spleens 24 hours after rapid injection with pCAGGS-rat CTLA4-Ig-Glu-tag into tail vein. Expressions of vector-derived CTLA4-Ig mRNA were similarly examined using the primers (5′-tctgactgaccgcgttactccca-3′ in sequences of pCAGGS, 5′-gtgaggttcactctgctttcatta-3′ in sequences of rat CTLA4) by LightCycler.

Statistical Analysis

Data obtained from quantitative reverse transcription-polymerase chain reaction, HW, BW, myocarditis area, and hemodynamic parameters were presented as the mean ± SD. Date of concentration of IL-1RA-Ig-Glu-tag were expressed as mean ± SEM. Statistical comparisons were performed by the Student non-paired t-tests or one-way analysis of variance and Bonferroni multiple comparison test. The differences were considered significant at $P < .05$.

Results

Plasma Rat CTLA4-Ig-Glu-tag Protein Levels

Plasma CTLA4-Ig-Glu-tag protein levels, calculated by using Glu-tag, increased, peaking at 3550 ± 336 ng/mL (mean ± SEM) on Day 1 after hydrodynamics-based gene delivery by naked plasmid vector, namely a rapid tail vein injection of a large volume of plasmid DNA solution. Levels were maintained until Day 16 (1810 ± 400 ng/mL on Day 4, 3090 ± 629 ng/mL on Day 7, 2590 ± 270 ng/mL on Day 10, 2980 ± 321 ng/mL on Day 13, and 2300 ± 397 ng/mL on Day 16). However, plasma CTLA4-Ig-Glu-tag

protein levels after a injection into the tibialis anterior muscles by electroporation were under 3.5 ng/mL, which was the sensitivity threshold, at all times (Fig. 1).

Vector-Derived CTLA4-Ig mRNA Expression in Various Organs

Because plasma CTLA4-Ig-Glu-tag protein levels were highest on Day 1 after hydrodynamics-based gene delivery, various organs were examined at the time. We detected the transgene-derived CTLA4-Ig mRNA by quantitative real-time polymerase chain reaction in the liver, heart, lungs, and kidney of rats that had been injected with a 20-mL volume of 800 μg of pCAGGS-rat CTLA4-Ig-Glu-tag (Fig. 2). Among the organs examined, the level of CTLA4-Ig gene expression in the liver was the highest.

CTLA4-Ig Treatment for EAM

EAM rats were treated with pCAGGS (control group, n = 9) or pCAGGS CTLA4-Ig (CTLA4 group, n = 9). The parameters measured on Day 17 were compared between the two groups and the results of the statistical analysis are summarized in Table 1 and displayed in Fig. 3–6. The results for HW, BW, and HW/BW are shown in Fig. 3. BW was larger, whereas HW and HW/BW were smaller in the CTLA4 group compared with the control group; these differences were all statistically significant ($P < .01$). The ratio of inflammatory area was significantly smaller ($P < .05$) in the CTLA4 group compared with the control group (Fig. 4A, 4B). There was no significant difference in heart rate between the two groups. However, the mean arterial pressure, left ventricular pressure, and the absolute value of +dP/dT or –dP/dT were significantly larger in the CTLA4 group compared with the control group ($P < .01$ in each case). Left ventricular end-diastolic pressure and central venous pressure were significantly smaller in the CTLA4 group compared with the control group ($P < .05$ for both) (Fig. 5).

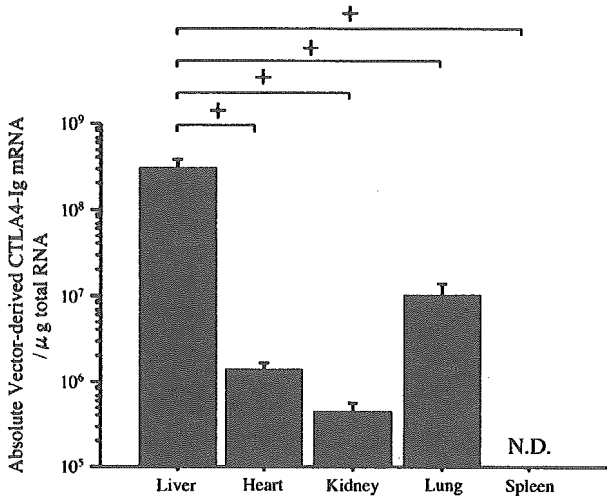

Fig. 2. Absolute vector-derived CTLA4-Ig mRNA per 1 μg total RNA in liver, heart, kidney, lung, and spleen of normal rat 24 hours after hydrodynamics-based gene delivery of pCAGGS-rat CTLA4-Ig-Glu-tag (n = 3). Each bar represents mean ± SD. $P <$ .01 differences between the 2 groups. Statistical comparisons were performed by one-way analysis of variance and Bonferroni multiple comparison test.

Expression of ANP mRNA in EAM Hearts

The expression of ANP mRNA in the heart is an important response in the modulation of cardiac function.[24] The level of ANP mRNA in the CTLA4 group ($0.80 \times 10^6 \pm 0.96 \times 10^6$ molecules/μg total mRNA) was significantly lower ($P < .01$) compared with levels in the control group ($7.70 \times 10^6 \pm 4.41 \times 10^6$ molecules/μg total mRNA) (Fig. 6).

Expression of IL-2 mRNA in Popliteal Lymph Node

EAM on Day 14 is thought to be in progress of myocarditis, and it was demonstrated that concanavalin A–activated

Table 1. Summary of Results in the Control and CTLA4 Groups

	Control (n = 9)	CTLA4 (n = 9)	*P* Value
HW (g)	1.11 ± 0.07	0.86 ± 0.18	<.01
BW (g)	218 ± 5.36	236 ± 14.1	<.01
HW/BW_1000	5.08 ± 0.42	3.73 ± 0.95	<.01
Inflammatory ratio (%)	38.6 ± 12.3	12.1 ± 13.91	<.05
Hemodynamic parameters			
HR (bpm)	377 ± 27.8	402 ± 25.3	
CVP (mm Hg)	5.93 ± 3.08	2.87 ± 1.12	<.05
AP (mm Hg)	76.8 ± 5.74	94.6 ± 11.6	<.01
LVP (mm Hg)	95.1 ± 7.73	117 ± 14.5	<.01
LVEDP (mm Hg)	11.7 ± 2.62	7.38 ± 3.28	<.05
dP/dT max	6034 ± 1344	8833 ± 1969	<.01
dP/dT min	−5654 ± 1147	−8069 ± 1266	<.01
mRNA of ANP (molecules/μg of total RNA)	$7.70 \times 10^6 \pm 4.41 \times 10^6$	$0.80 \times 10^6 \pm 0.96 \times 10^6$	<.01

Statistical significance between the control group and CTLA4 group was determined by the Student's non-paired *t* test.

HW, heart weight; BW, body weight; HR, heart rate; CVP, central venous pressure; AP, arterial pressure; LVP, left ventricular pressure; LVEDP, left ventricular end-diastolic pressure; dP/dT, rate of intraventricular pressure rise and decline; ANP, atrial natriuretic peptide.

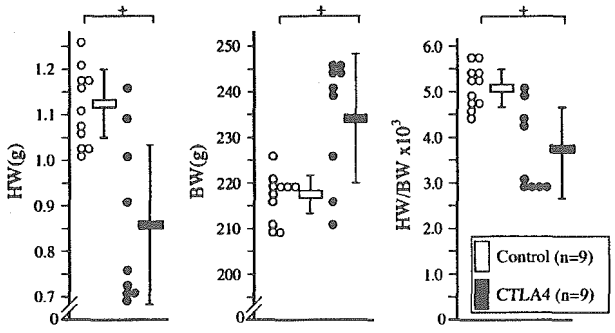

Fig. 3. Effects of pCAGGS-CTLA4-Ig on body weight (BW), heart weight (HW), and HW/BW ratio on Day 17 after immunization. Each bar represents mean ± SD. $P < .01$ differences between the 2 groups. Statistical comparisons were performed by the Student non-paired t-tests.

T cells in lymph node on Day 14 elicited severe myocarditis.[3] mRNA of IL-2 known as T-cell growth factor was significantly suppressed by hydrodynamics-based gene delivery of pCAGGS rat CTLA4-Ig (Fig. 7).

Discussion

We examined the effect of CTLA4-Ig on EAM using gene therapy with naked plasmid vector. We found that CTLA4-Ig improved dramatically not only the histopathologic finding, but also cardiac function of EAM. In previous studies, we have investigated the protective effect of antibody for TCR and cytokines in EAM.[2,25] This therapy has the advantage that specific immunologic tolerance can be achieved by blocking costimulatory signals in spite of lack of exact information of the autoantigen. Blockade of the CD28-B7 pathway with CTLA4-Ig has been demonstrated previously as a useful strategy in autoimmune disease.[26-29] In this study, it was demonstrated that gene expression of IL-2 in EAM popliteal lymph node was suppressed by CTLA4-Ig. IL-2, known as a Th1 cytokine, is thought to play an important role in progression of EAM.[30] This suppression of IL-2 mRNA may be one of the mechanism of CTLA4-Ig effect.

The CTLA4-Ig chimeric protein consists of rat CTLA4 and rat IgG1 Fc portions and Shioji reported that a large amount of the immunoglobulin Fc portions were effective for the prevention of EAM.[31] However, in this study, the serum

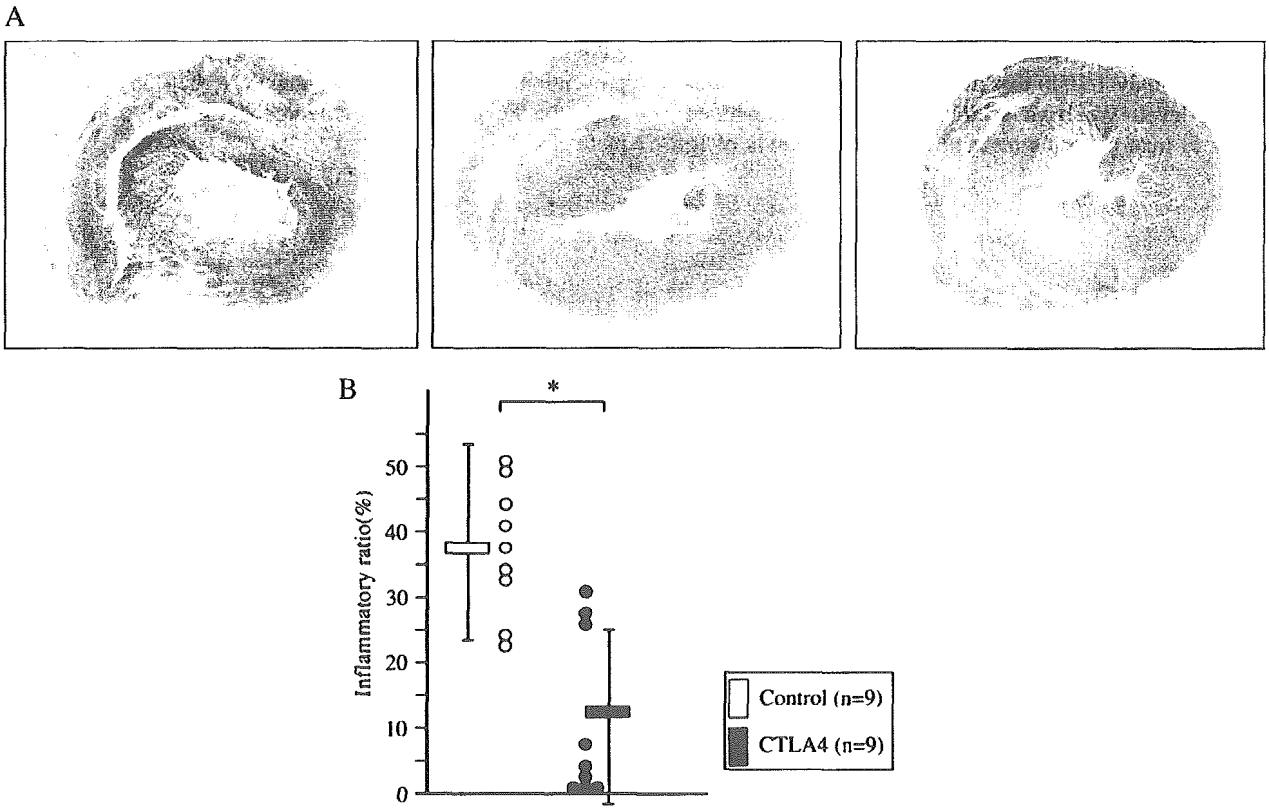

Fig. 4. (A) Transverse section of hearts. No therapy group (left), pCAGGS-treated control group (middle), pCAGGS-CTLA4 Ig-treated group (right). Azan-Mallory staining. (B) The ratio of inflammatory area to whole section in the control group and CTLA4 group. Each bar represents mean ± SD. $P < .01$ differences between the 2 groups. Statistical comparisons were performed by the Student non-paired t-tests.

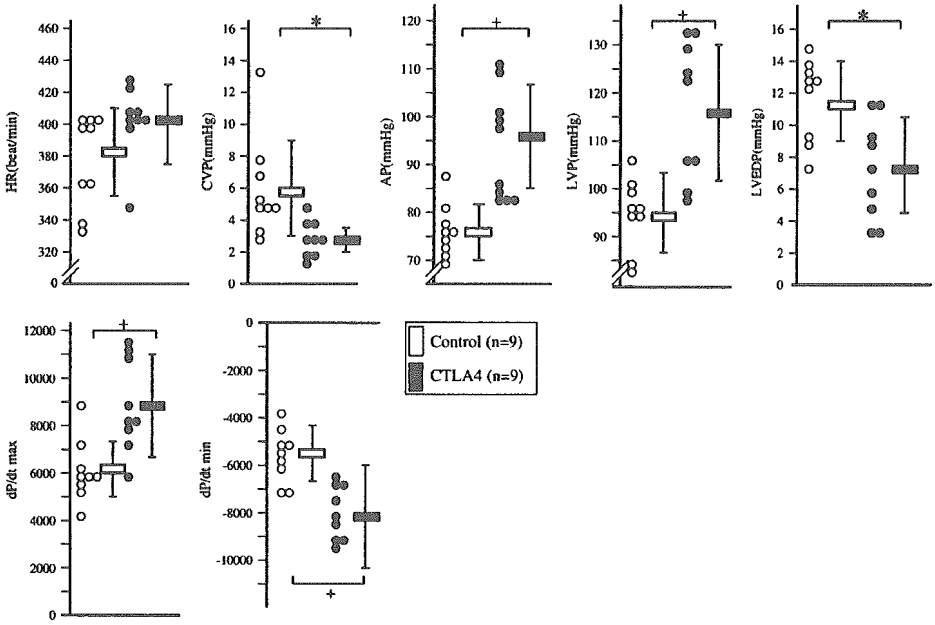

Fig. 5. Hemodynamic parameters on Day 17 after immunization. Each bar represents mean ± SD. Statistical comparisons were performed by the Student non-paired t-tests. $^*P < .05$, $P < .01$ differences between the 2 groups. HR (heart rate); CVP (central venous pressure); AP (arterial pressure); LVP (left ventricular pressure); LVEDP (left ventricular end-diastolic pressure); dP/dT (rate of intraventricular pressure rise and decline).

level of CTLA4-Ig achieved by hydrodynamics-based transfection was only 1/1000 that of the native serum immunoglobulin level. We have used the hydrodynamics-based method to treat plasmids inserted into various kinds of Ig chimeric protein, but some therapies were ineffective in the prevention of EAM (data not shown). In the study reported here, the Fc portion of immunoglobulin was considered ineffective.

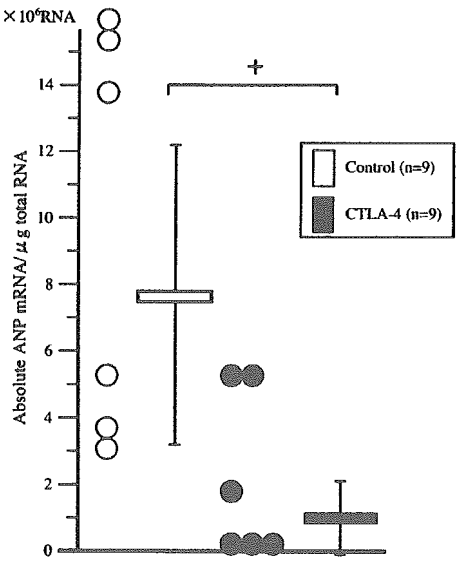

Fig. 6. Absolute number of atrial natriuretic peptide (ANP) mRNA per 1 μg of total RNA in the 2 groups. Each bar represents mean ± SD. $P < .01$ differences between the 2 groups. Statistical comparisons were performed by the Student non-paired t-tests.

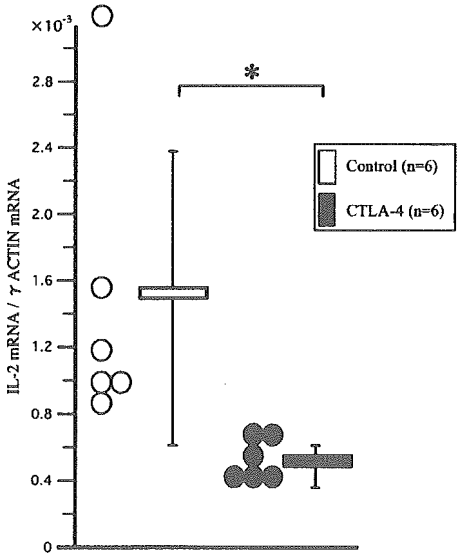

Fig. 7. Copy numbers of IL-2 mRNA/copy numbers of γ-actin in popliteal lymph nodes of the 2 groups. Each bar represents mean ± SD. $^*P < .05$ differences between the 2 groups. Statistical comparisons were performed by the Student non-paired t-tests.

Previous studies demonstrated that the intravenous administration of adenoviral vectors encoding a CTLA4-Ig chimeric protein could successfully ameliorate experimental allergic encephalomyelitis,[32] murine systemic lupus erythematosus,[33] murine collagen-induced arthritis,[34] nephritis in a murine lupus model,[35] and EAM.[10] Gene therapy by adenoviral vector is a powerful technology. However, compared with virus-mediated gene transfer systems, the introduction of an exogenous gene into cells in the form of naked DNA has many obvious advantages. Preparation of DNA has become routine in many laboratories and because it is chemically and biologically stable, no sophisticated storage conditions are required. Large quantities of highly purified plasmid DNA can be obtained easily and inexpensively. Wolff et al reported the successful expression of a reporter gene in muscle[15] and Aihara and Miyazaki reported that gene transfer into muscle by electroporation in vivo was 100 times more efficient than simple intramuscular DNA injection.[36] We first examined the effect on EAM of CTLA4-Ig gene transfer into muscle by electroporation. However, its effect was weak, and hemodynamic differences between the control group and CTLA4 group were not significant (data not shown). Therefore, in the current study, we tried hydrodynamics-based transfection and have demonstrated that it clearly prevented the development of EAM. Plasma CTLA4-Ig-Glu-tag protein levels by hydrodynamics-based transfection were about 1000 times higher than by intramuscular transfection with electroporation. We demonstrated that the transgene-derived CTLA4-Ig mRNA was detected by quantitative real-time polymerase chain reaction in the liver, heart, lungs, spleen, and kidney of rats that had been treated with hydrodynamic-based transfection. Among the organs examined, the level of CTLA4-Ig gene expression in the liver was the highest. Hydrodynamics-based transfection is an easy and powerful technology. There was no significant difference in the hemodynamics on Day 17 after immunization between the control group and nontreated EAM group (data not shown), which indicates that the initial temporal volume overload did not affect the hemodynamic status of EAM. This technology remedies the shortcoming of gene transfection using adenovirus, as outlined previously. Matsui et al demonstrated therapy with adenovirus vectors containing CTLA4-Ig to EAM.[10] In their study, blockade of T-cell costimulation by CTLA4-Ig prevented the induction and progression of EAM, as shown in their histologic findings, HW/BW ratio, and cellular and hormonal immune response. Our data also indicated that a therapeutic administration of pCAGGS-CTLA4Ig prevented the induction of EAM, and improved not only the histologic findings, but also the hemodynamic status. Five of the 9 rats in the CTLA4-Ig group had few or no inflammatory findings. These results together suggest that pCAGGS-CTLA4-Ig is as effective as adenovirus vector in preventing the induction of EAM.

We demonstrated that intravenous injections of plasmids with cDNA encoding CTLA4-Ig protected Lewis rats from developing EAM as evidenced by a significant reduction to the histologic cardiac cellular infiltrate and an improvement in the hemodynamic status.

References

1. Kodama M, Matsumoto Y, Fujiwara M, Masani F, Izumi T, Shibata A. A novel experimental model of giant cell myocarditis induced in rats by immunization with cardiac myosin fraction. Clin Immunol Immunopathol 1990;57:250–62.
2. Hanawa H, Kodama M, Inomata T, Izumi T, Shibata A, Tuchida M, et al. Anti-alpha beta T cell receptor antibody prevents the progression of experimental autoimmune myocarditis. Clin Exp Immunol 1994;96: 470–5.
3. Kodama M, Matsumoto Y, Fujiwara M. In vivo lymphocyte-mediated myocardial injuries demonstrated by adoptive transfer of experimental autoimmune myocarditis. Circulation 1992;85:1918–26.
4. Jorgensen JL, Reay PA, Ehrich EW, Davis MM. Molecular components of T-cell recognition. Annu Rev Immunol 1992;10:835–73.
5. Schwartz RH. A cell culture model for T lymphocyte clonal anergy. Science 1990;248:1349–56.
6. Shahinian A, Pfeffer K, Lee KP, Kundig TM, Kishihara K, Wakeham A, et al. Differential T cell costimulatory requirements in CD28-deficient mice. Science 1993;261:609–12.
7. Harding FA, McArthur JG, Gross JA, Raulet DH, Allison JP. CD28-mediated signalling co-stimulates murine T cells and prevents induction of anergy in T-cell clones. Nature 1992;356:607–9.
8. Linsley PS, Ledbetter JA. The role of the CD28 receptor during T cell responses to antigen. Annu Rev Immunol 1993;11:191–212.
9. Lenschow DJ, Zeng Y, Thistlethwaite JR, Montag A, Brady W, Gibson MG, et al. Long-term survival of xenogeneic pancreatic islet grafts induced by CTLA4Ig. Science 1992;257:789–92.
10. Matsui Y, Inobe M, Okamoto H, Chiba S, Shimizu T, Kitabatake A, et al. Blockade of T cell costimulatory signals using adenovirus vectors prevents both the induction and the progression of experimental autoimmune myocarditis. J Mol Cell Cardiol 2002;34:279–95.
11. Pauschinger M, Bowles NE, Fuentes-Garcia FJ, Pham V, Kuhl U, Schwimmbeck PL, et al. Detection of adenoviral genome in the myocardium of adult patients with idiopathic left ventricular dysfunction. Circulation 1999;99:1348–54.
12. Yang Y, Li Q, Ertl EH, Wilson JM. Cellular and humoral immune responses to viral antigens create barriers to lung-directed gene therapy with recombinant adenoviruses. J Virol 1995;69:2004–15.
13. Somia N, Verma IM. Gene therapy: trials and tribulations. Nat Rev Genet 2000;1:91–9.
14. Hickman MA, Malone RW, Lehmann-Bruinsma K, Sih TR, Knoell D, Szoka FC, et al. Gene expression following direct injection of DNA into liver. Hum Gene Ther 1994;5:1477–83.
15. Wolff JA, Malone RW, Williams P, Chong W, Acsadi G, Jani A, et al. Direct gene transfer into mouse muscle in vivo. Science 1990; 247:1465–8.
16. Jiang J, Yamato E, Miyazaki J. Intravenous delivery of naked plasmid DNA for in vivo cytokine expression. Biochem Biophys Res Commun 2001;289:1088–92.
17. Liu F, Song Y, Liu D. Hydrodynamics-based transfection in animals by systemic administration of plasmid DNA. Gene Ther 1999;6:1258–66.
18. Maruyama H, Higuchi N, Nishikawa Y, Kameda S, Iino N, Kazama JJ, et al. High-level expression of naked DNA delivered to rat liver via tail vein injection. J Gene Med 2002;4:333–41.
19. Hou D, Maclaughlin F, Thiesse M, Panchal VR, Bekkers BC, Wilson EA, et al. Widespread regional myocardial transfection by plasmid encoding Del-1 following retrograde coronary venous delivery. Catheter Cardiovasc Interv 2003;58:207–11.
20. Hanawa H, Watanabe R, Hayashi M, Yoshida T, Abe S, Komura S, et al. Novel method for assay of protein in blood after intravenous injection of plasmid DNA. Tohoku J Exp Med 2004;202:155–61.